Chapter 2: Mathematical description

As exposed in the introduction section, several models are proposed in literature to deal with geomorphical changes induced by unsteady flows. In the present thesis two approaches are presented: The most often used model, based on the Saint-Venant – Exner equations (for example Cunge et al., 1980) and a more recently developed approach, a two-layer model instigated by Capart (2000). In order to underline the differences between the two-layer and the classical approaches, the mathematical description of both existing models is proposed. First the assumptions and equations of each model are exposed, as well in the case of the Saint-Venant – Exner as in the case of the various versions of the two layer model (depending on the assumptions). Then, the eigenstructure of those equations is analysed and a new two-layer Froude number is proposed. It reveals particularly useful to study in which way information propagates and to give the essential basis to understand the numerical resolution, essentially the boundary conditions treatment.

In the following, a one-dimensional approach based on a unit width is adopted. This limitation has no incidence as the experiments to model concern one-dimensional flows.

2.1. Governing equations

2.1.1. Saint-Venant – Exner

To take into account the presence of sediments, the Saint-Venant equations were completed to obtain the Saint-Venant – Exner equations demonstrated for example by Cunge et al (1980) and Sloff (1993). Assuming the shallow-water hydrostatic pressure distribution, the flow is composed of three parts as pictured in Figure 2.1.

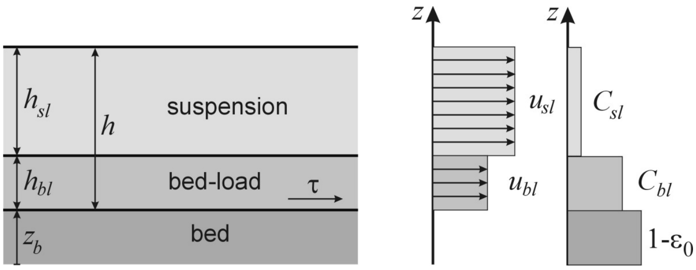

Figure 2.1. Saint-Venant – Exner stratified flow

Water has a volumetric mass ρ_w and sediments have a volumetric mass ρ_s and a porosity ε_0.

The upper part of the flow is the suspended sediment transport zone characterised by a depth h_{sl} and by a mean volumetric concentration in sediment C_{sl}.

$$C_{sl} = \frac{1}{h_{sl}} \int_{h_{sl}} C\,dh = \frac{1}{h_{sl} u_{sl}} \int_{h_{sl}} Cu\,dh \tag{2.1}$$

where C is the local concentration in sediment and the subscript *sl* means related to the suspension layer. In this case, as the velocity is supposed uniform in each section, the volumetric concentration is identical to the discharge concentration. The velocity of the suspended sediments is assumed to be identical to the velocity of water u_{sl} in this part. The total discharge (sediment and water) $q_{sl\ w+s} = h_{sl} u_{sl}$ is composed of the suspended sediment discharge $q_{sl\ s} = C_{sl} h_{sl} u_{sl}$ and the water discharge $q_{sl\ w} = (1 - C_{sl}) h_{sl} u_{sl}$.

The intermediate part of the flow is the bed-load sediment transport zone of depth h_{bl}, the subscript *bl* means related to the bed-load layer. It is composed of sediment with a mean volumetric concentration C_{bl} calculated in the same way as the mean volumetric concentration C_{sl} in the suspension part (2.1). Sediments are supposed to move at the same velocity than water u_{bl}, which is lower than u_{sl}. The total discharge in this part of the flow $q_{bl\ w+s} = h_{bl} u_{bl}$ is divided between the bed-load sediment discharge $q_{bl\ s} = C_{bl} h_{bl} u_{bl}$ and the water discharge $q_{bl\ w} = (1 - C_{bl}) h_{bl} u_{bl}$.

The lower part of the flow is composed of non-moving saturated sediment presenting a porosity ε_0 corresponding to a concentration in sediment of (1 - ε_0).

Exchanges of sediment and water are possible between these three zones. When sediment transport rate changes from suspension to bed-load or inversely, there is an exchange between the suspended sediment transport and the bed-load transport zones. When erosion occurs, sediments from the non-mobile bed migrate to the bed-load transport zone. Conversely, when there is a deposition, sediments in movement in the bed-load transport zone settle on the fixed bed, which implies a displacement of the interface z_b.

The terms quantifying these exchanges are quite difficult to treat, to avoid the expression of these terms, the mass and momentum conservations are written on a control volume (dotted line) containing the three parts described previously (Fig.2.2).

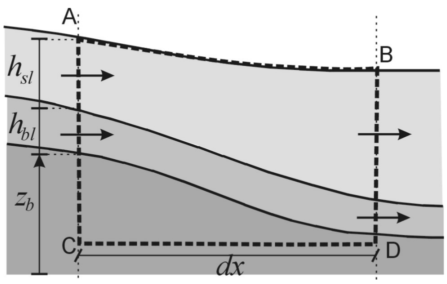

Figure 2.2. Saint-Venant – Exner control volume

The mass conservation applied on the mixture flow (sediment and water) on the control volume ABCD is

$$\frac{\partial\left(h_{sl}+h_{bl}+z_b\right)}{\partial t}+\frac{\partial\left(h_{sl}u_{sl}+h_{bl}u_{bl}\right)}{\partial x}=0 \tag{2.2}$$

where the total discharge is

$$h_{sl}u_{sl}+h_{bl}u_{bl}=q_{sl\ w+s}+q_{bl\ w+s}=q_{w+s} \tag{2.3}$$

The problem to solve is assumed to be equivalent to a simplified one, where the two zones of suspension and bed-load transport are mixed together, in such a way that the stratified flow in Figure 2.1 is simplified as in Figure 2.3.

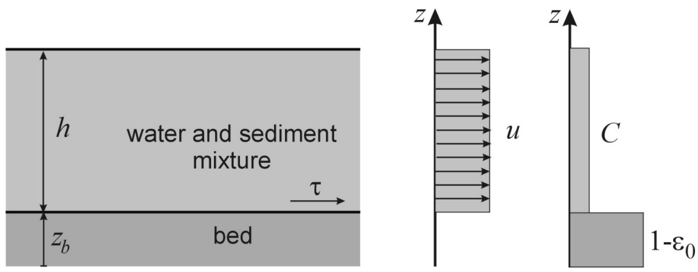

Figure 2.3. Saint-Venant – Exner mixed flow

The total depth of the mixture is

$$h = h_{sl} + h_{bl} \tag{2.4}$$

and the mean velocity and concentration of the mixture are

$$u = \frac{h_{sl}u_{sl} + h_{bl}u_{bl}}{h} \qquad C = \frac{h_{sl}C_{sl} + h_{bl}C_{bl}}{h} \tag{2.5a-b}$$

Under definitions (2.4) and (2.5a), expression (2.2) can be written

$$\frac{\partial h}{\partial t} + \frac{\partial z_b}{\partial t} + \frac{\partial hu}{\partial x} = 0 \tag{2.6}$$

The mass conservation applied on the sediment phase on the control volume ABCD (Fig.2.2) is

$$\frac{\partial\left(h_{sl}C_{sl} + h_{bl}C_{bl} + z_b\left(1-\varepsilon_0\right)\right)}{\partial t} + \frac{\partial\left(h_{sl}u_{sl}C_{sl} + h_{bl}u_{bl}C_{bl}\right)}{\partial x} = 0 \tag{2.7}$$

Where the solid discharge is

$$h_{sl}u_{sl}C_{sl} + h_{bl}u_{bl}C_{bl} = q_{sl\ s} + q_{bl\ s} = q_s \tag{2.8}$$

Under definitions (2.4) and (2.5), expression of the sediment mass conservation (2.7) can be written

$$\frac{\partial hC}{\partial t} + (1-\varepsilon_0)\frac{\partial z_b}{\partial t} + \frac{\partial q_s}{\partial x} = 0 \qquad (2.9)$$

The momentum conservation applied on the mixture flow on the control volume ABCD is identical to the one obtained in pure hydrodynamics except the fact it is applied on the water-sediment mixture, whose volumetric mass is

$$\rho_m = \rho_w(1-C) + \rho_s C \qquad (2.10)$$

The momentum equation becomes

$$\frac{\partial hu}{\partial t} + \frac{\partial}{\partial x}\left(hu^2 + \tfrac{1}{2} gh^2\right) + gh\frac{\partial z_b}{\partial x} = -\frac{\tau}{\rho_m} \qquad (2.11)$$

where τ is the shear stress applied to the bed. This system of three equations (2.6), (2.9) and (2.11) contains six unknowns : h, u, z_b, τ, q_s and C. Three additional relations are proposed to calculate q_s, τ and C in order to close the system.

The first relation expresses the friction shear stress τ applied on the non-mobile bed (Figs.2.1 and 2.3).

$$\tau = \rho_m g R_b S_f \qquad (2.12)$$

where R_b is the hydraulic radius related to the bed : in case of unit width (bank effects are neglected) it is equivalent to the hydraulic radius $R = R_b = h$. The friction slope S_f can be deduced, for instance, from the Manning uniform flow relation.

$$S_f = \frac{n^2 u^2}{R^{4/3}} \qquad (2.13)$$

where n is the Manning roughness coefficient.

The second relation is a solid transport formula chosen among the various formulae proposed in the literature. The selected formula has to be appropriate to the kind of solid transport to model (suspension and/or bed-load). In the present work, only bed-load sediment transport is concerned and the formula proposed by Meyer-Peter and Müller (1948) is considered.

$$q_s = 8\sqrt{g(s-1)d^3}\left(\left(\frac{n_b'}{n_b}\right)^{3/2}\frac{\gamma_w R_b S_f}{(\gamma_s-\gamma_w)d}-0.047\right)^{3/2} \tag{2.14}$$

where q_s is the solid discharge in m³/s/m, $s = \rho_s/\rho_w$ is the relative density of the sediments, d is the mean diameter of the sediments, n_b is the Manning roughness coefficient corresponding to the bed, n'_b is the Manning roughness coefficient taking grain roughness into account (if no bed forms occurs, the ratio $n'_b/n_b = 1$), γ_w and γ_s are respectively the water and the bed volumetric weight.

The third expression links the concentration of sediment in the mixture as the ratio between the solid and the total (sediment + water) discharge.

$$C = \frac{q_s}{q_{w+s}} \tag{2.15}$$

Some assumptions are usually made to simplify equations (2.6), (2.7) and (2.11). The variation in time of the bed level is assumed negligible in comparison with the variation in time of the water depth in (2.6).

$$\frac{\partial z_b}{\partial t} << \frac{\partial h}{\partial t} \tag{2.16}$$

The mean concentration C is assumed to be very low, because the amount of sediment in the mixed flow is very low in comparison with the amount of water. The variation of the amount of sediment with time is neglected in (2.7)

$$\frac{\partial hC}{\partial t} << \frac{\partial z_b}{\partial t} \tag{2.17}$$

Under these assumptions, equations (2.6) and (2.7) simplify

$$\frac{\partial h}{\partial t}+\frac{\partial hu}{\partial x}=0 \tag{2.18}$$

$$(1-\varepsilon_0)\frac{\partial z_b}{\partial t}+\frac{\partial q_s}{\partial x}=0 \tag{2.19}$$

In order to make the mean velocity u as a main variable, the momentum equation (2.11) can be written by combination with (2.18)

$$\frac{\partial u}{\partial t}+\frac{\partial}{\partial x}\left(\tfrac{1}{2}u^2+g(z_b+h)\right)=-\frac{\tau}{\rho_m h}=-gS_f \tag{2.20}$$

The variables h and u are related to the mixture flow, they do not have to be associated to the water phase. Nevertheless, some authors assumed the participation of sediment is limited in comparison with the participation of water and consider these variables as hydrodynamic variables.

The system of equations (2.6), (2.7) and (2.11) can be rewritten under a vector formulation.

$$\frac{\partial \mathbf{U}}{\partial t}+\frac{\partial \mathbf{F}(\mathbf{U})}{\partial x}=\mathbf{S}(\mathbf{U}) \tag{2.21}$$

where $\mathbf{U}=\begin{pmatrix} h \\ u \\ z_b \end{pmatrix}$ $\quad \mathbf{F}(\mathbf{U})=\begin{pmatrix} hu \\ \frac{1}{2}u^2+g(z_b+h) \\ \frac{1}{1-\varepsilon_0}q_s \end{pmatrix} \quad \mathbf{S}(\mathbf{U})=\begin{pmatrix} 0 \\ -gS_f \\ 0 \end{pmatrix}$ (2.22)

2.1.2. Two-layer model

As an alternative to common approaches based on the Saint-Venant – Exner equations, a two-layer model, developed at the origin by Capart (2000), is proposed to calculate morphodynamic evolutions. Assuming the shallow-water hydrostatic pressure distribution, the flow is divided in two layers constituted of incompressible fluid. The upper layer is constituted of clear water and the lower one, called the sediment transport layer, is a water-sediment mixture assumed to behave like a fluid. An interaction between the transport layer and the bed allows to take into account erosion and/or deposition. Several variants of the model depending on alternative assumptions are exposed. First, Capart (2000) proposed a basic two-layer model assuming identical velocity in both water and sediment transport layers and similar sediment concentration in the transport layer and in the bed. Then, Capart and Young (2002) improved this model allowing the velocity of each layer to be distinct. Finally, Spinewine (2005) took into account that the sediment concentration in the sediment transport layer is lower than in the bed. In some particular flow conditions, the previous model may lose its hyperbolic character. In order to tackle this problem, an adaptation of the model is proposed. These four variants of the model are exposed. All are deduced from the same process based on the continuity and momentum equations and on friction laws at the interfaces. The demonstration of the most elaborate of the models cited above (two-velocity, two-concentration) is developed, for more details see Spinewine (2005). The equations corresponding to the other three variants are easily deduced.

2.1.2.1. Two-velocity two-concentration model

The two-layer model already demonstrated in Spinewine (2005) is detailed here. The main variables are the thickness of the water layer h_w and of the transport layer h_s, the velocity in each layer u_w and u_s, respectively, and the level of the interface between the transport layer and the bed z_b (Fig. 2.4).

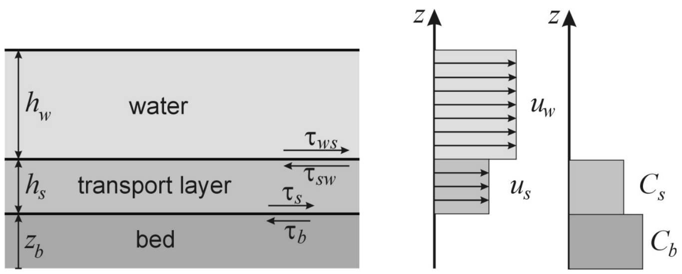

Figure 2.4. Two-velocity two-concentration model

The transport layer and the fixed bed are constituted of a water-sediment mixture, only bed load is modelled. The sediment concentration in the bed is defined as $C_b = 1 - \varepsilon_0$, which leads to the volumetric mass of the bed $\rho_b' = (1 - C_b)\rho_w + C_b\,\rho_s$, where ρ_w and ρ_s are the water and the grain density, respectively. As the sediment mobilisation requires a decrease in concentration ($C_s < C_b$), the transport layer volumetric mass $\rho_s' = (1 - C_s)\rho_w + C_s\,\rho_s$ is lower than in the bed. The velocity in the transport layer is allowed to be distinct from the velocity in the water layer, but both velocities are assumed to be uniform in their layer. Erosion and deposition induce a mass exchange occurring between the bed and the transport layer, at the interface defined by the level z_b. The erosion rate e_b is defined as the evolution of the interface level z_b with time

$$e_b = -\frac{\partial z_b}{\partial t} \tag{2.23}$$

Moreover, during erosion and deposition processes, mass exchange has to be taken into account at the interface between the water and the transport layers defined by the level $z_s = z_b + h_s$. This exchange is due to the change in sediment concentration between the bed and the transport layer ($C_s < C_b$). The associated displacement of the interface z_s with time defines e_s

$$e_s = -\frac{\partial z_s}{\partial t} \tag{2.24}$$

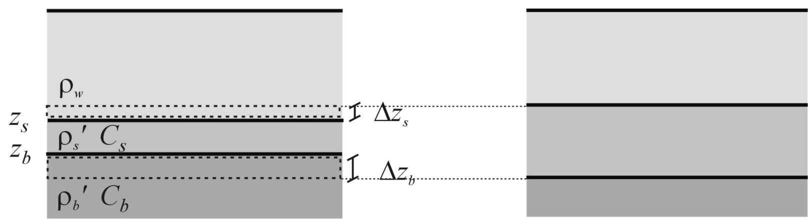

Figure 2.5. Two-velocity two-concentration model: erosion

In case of erosion, the erosion rate is positive and the variation of the bed level Δz_b is negative. A part of the bed becomes a part of the transport layer (Fig.2.5). The mass corresponding to Δz_b in the bed $\rho_b'\Delta z_b$ becomes, in the transport layer, $\rho_s'\Delta z_b$. There is a loss of mass, which is deduced from the difference between the mass of the trench Δz_b after and before erosion.

$$\Delta z_b(\rho_b' - \rho_s') \tag{2.25}$$

In case of erosion, e_s and the variation of the transport layer level Δz_s are positive. A part of the water layer becomes a part of the transport layer (Fig.2.5). The mass corresponding to Δz_s in the water layer $\rho_w \Delta z_s$ becomes, in the transport layer, $\rho_s' \Delta z_s$. There is a gain of mass, which is deduced from the difference between the mass of the trench Δz_s after and before erosion.

$$\Delta z_s(\rho_s' - \rho_w) \tag{2.26}$$

Expressions (2.25) and (2.26) remain identical in case of deposition (Fig.2.6), only the sign of Δz_b and Δz_s is affected.

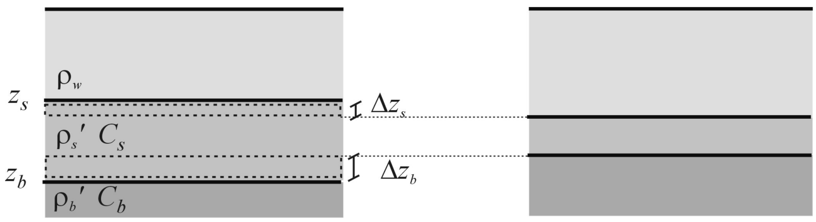

Figure 2.6. Two-velocity two-concentration model: deposition

As the mass of the system has to be conserved during the erosion and deposition processes, the loss (2.25) and the gain (2.26) of mass have to be identical

$$\Delta z_b(\rho_b' - \rho_s') = \Delta z_s(\rho_s' - \rho_w) \tag{2.27}$$

A link between the movement of both interfaces can be deduced

$$\begin{aligned} \frac{\Delta z_s}{\Delta z_b} &= -\frac{e_s}{e_b} = \frac{\rho_b' - \rho_s'}{\rho_s' - \rho_w} \\ &= \frac{((1-C_b)\rho_w + C_b\rho_s) - ((1-C_s)\rho_w + C_s\rho_s)}{((1-C_s)\rho_w + C_s\rho_s) - \rho_w} = \frac{C_b - C_s}{C_s} \end{aligned} \tag{2.28}$$

which gives the expression of e_s as a function of the erosion rate e_b considering the volumetric mass or the sediment concentration of each layer

$$e_s = -\frac{\rho_b' - \rho_s'}{\rho_s' - \rho_w} e_b = -\frac{C_b - C_s}{C_s} e_b \tag{2.29}$$

The signs of e_s and e_b are opposite, e_b is positive in case of erosion and negative in case of deposition.

If the sediment concentration in the transport layer is close to the experimentally observed value, the computed transport layer depth and velocity can be compared to real values. However, if the sediment concentration is not appropriate, only the solid discharge keeps a physical meaning. If the sediment discharge is too low, the assumption of a bed load layer is less appropriate. In this case, the thickness and velocity of this layer are not physically representative.

Interface movement and vertical velocity

A small control volume of sediment around the interface z_b is considered, containing a thin part of the transport layer and a thin part of the fixed bed (Fig. 2.7). The control volume moves with the vertical velocity corresponding to the velocity of the interface $\partial z_b / \partial t = -e_b$.

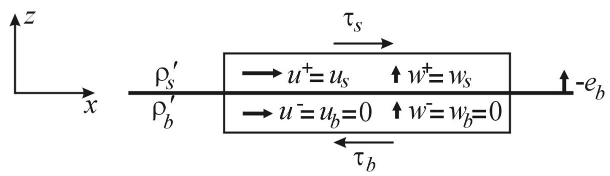

Figure 2.7. Control volume around the interface z_b, applied shear stresses

The mass conservation on the control volume writes

$$\sum \rho \left(\mathbf{V}_r \mid d\mathbf{A} \right) = 0 \tag{2.30}$$

where $\mathbf{V_r}$ is the relative (to the interface) velocity vector and $d\mathbf{A}$ is the surface vector. The relative velocity of the flow crossing a mobile interface is the difference between the absolute normal component of the flow velocity and the absolute velocity of the mobile interface. In the present case, the absolute z-component of the velocity in the bed $w^- = w_b$ is equal to zero as the sediments are not moving. The absolute z-component of the velocity in the transport layer $w^+ = w_s$ can be deduced from the mass conservation (2.30).

$$\left(\rho_s'\left(w^+ - \frac{\partial z_b}{\partial t}\right) - \rho_b\left(w^- - \frac{\partial z_b}{\partial t}\right)\right)dx\,dy \\ = \left(\rho_s'\left(w_s + e_b\right) - \rho_b\left(w_b + e_b\right)\right)dx\,dy = 0 \tag{2.31}$$

$$w_s = \frac{\rho_b' - \rho_s'}{\rho_s'} e_b = -\frac{\rho_s' - \rho_w}{\rho_s'} e_s \tag{2.32}$$

This vertical velocity in the transport layer is due to the variation of the sediment concentration between the bed and the transport layer.

The momentum equation in the x-direction writes:

$$\sum d\mathbf{F}_x = \sum \rho u \left(\mathbf{V}_r \mid d\mathbf{A}\right) \tag{2.33}$$

where $d\mathbf{F}$ is the elementary force acting on a boundary (volumetric forces are neglected because of higher order terms) and u is the velocity in the x-direction. Above the interface (Fig.2.7), the x-component of the velocity u^+ is the velocity of the transport layer u_s. Under the interface, the x-component of the velocity u^- is equal to zero, as this part of the bed is fixed. Developing (2.33) gives:

$$\left(\tau_s - \tau_b\right)dx\,dy = \left(\rho_s'\left(w^+ - \frac{\partial z_b}{\partial t}\right)u^+ - \rho_b'\left(w^- - \frac{\partial z_b}{\partial t}\right)u^-\right)dx\,dy \\ = \rho_s'\left(w_s + e_b\right)u_s\,dx\,dy \tag{2.34}$$

Substituting the expression of the vertical velocity in the transport layer w_s (2.32), the erosion rate e_b is deduced

$$e_b = -\frac{\partial z_b}{\partial t} = \frac{\tau_s - \tau_b}{\rho_b' u_s} \tag{2.35}$$

Identically, a small control volume around the interface z_s containing a thin part of the water layer and a thin part of the transport layer (Fig.2.8).

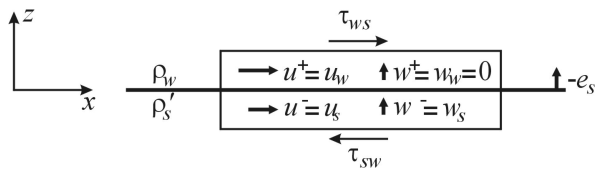

Figure 2.8. Control volume around the interface z_s, applied shear stresses

The mass conservation (2.30) applied on this control volume

$$\left(\rho_s'\left(w^- - \frac{\partial z_s}{\partial t}\right) - \rho_w\left(w^+ - \frac{\partial z_s}{\partial t}\right)\right)dx\,dy$$
$$= \left(\rho_s'(w_s + e_s) - \rho_w(w_w + e_s)\right)dx\,dy = 0 \tag{2.36}$$

By substituting the relation between the interface velocity e_s and the erosion rate (2.29) and the expression of the vertical velocity in the transport layer w_s (2.32), the absolute vertical velocity in water $w^+ = w_w$ can be deduced

$$w_w = 0 \tag{2.37}$$

The momentum equation (2.33) applied to the control volume (Fig.2.8) yields

$$(\tau_{ws} - \tau_{sw})dx\,dy = \left(\rho_w\left(w^+ - \frac{\partial z_s}{\partial t}\right)u^+ - \rho_s'\left(w^- - \frac{\partial z_s}{\partial t}\right)u^-\right)dx\,dy$$
$$= \left(\rho_w(w_w + e_s)u_w - \rho_s'(w_s + e_s)u_s\right)dx\,dy \tag{2.38}$$

By substituting the vertical velocity w_s (2.32) expressed as a function of e_s, using the relation (2.29) linking e_b and e_s, a new expression of e_s is available.

$$e_s = -\frac{\partial z_s}{\partial t} = \frac{\tau_{ws} - \tau_{sw}}{\rho_w(u_w - u_s)} \tag{2.39}$$

According to this expression, if e_s is different from zero (in case of erosion or deposition), the shear stress applied by the water layer on the sediment layer τ_{ws} is different from the resisting shear stress τ_{sw}.

Control volume

In order to develop mass and momentum conservation relations, a control volume with mobile boundaries has to be defined on each layer (Fig.2.9).

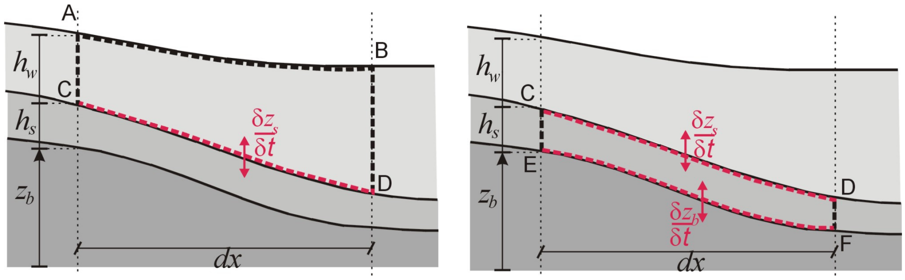

Figure 2.9. Water and transport layer control volumes (mobile boundaries in red)

The exact position of the control volume boundaries has an important influence for the following. The interfaces z_b and z_s correspond to discontinuities in volumetric mass $(\rho_w \neq \rho_s' \neq \rho_b')$, velocity $(u_w \neq u_s \neq u_b$ and $w_w \neq w_s \neq w_b)$ and shear stresses $(\tau_{ws} \neq \tau_{sw}$ and $\tau_s \neq \tau_b)$. It is not obvious to determine which parameters to chose in order to calculate mass and momentum exchanges through the control volume boundary if it is positioned precisely at an interface. That explains why the control volume boundaries have to be defined at an infinitely small distance ε above or below the interfaces.

In the case of the water control volume ABCD (Fig.2.9), the control boundary CD has to be above $(z_s + \varepsilon)$ or below $(z_s - \varepsilon)$ the interface z_s (Fig. 2.10). The boundary CD is moving vertically at the rate $\partial z_s / \partial t$ in case of erosion or deposition. If the upper limit is chosen, as it is located in the water layer, the parameters related to this layer are considered to calculate the exchanges across the boundary CD.

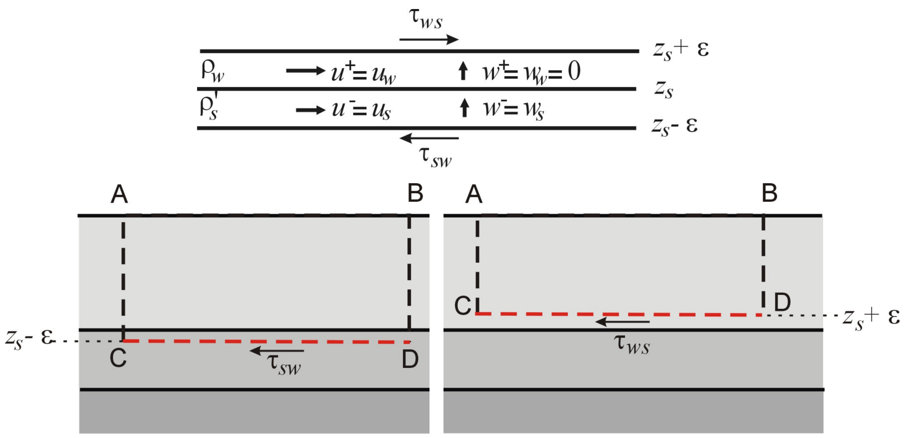

Figure 2.10. Interface z_s and water layer control volume definition (mobile boundaries in red)

In this case the external shear stress applied on the control surface CD is τ_{ws}, while it becomes τ_{sw} when the lower limit, located in the transport layer, is chosen. An expression based on the Chézy relation is proposed further for τ_{ws}, contrarily to τ_{sw} for which no simple relation is available. Then, in the following, it is chosen to fit the control volume boundary CD with the upper limit ($z_s + \varepsilon$) (Fig. 2.10). It is possible to demonstrate that the result is not affected by such a choice. Identically, several positions are possible for the boundaries of the sediment transport control volume CDEF (Fig 2.11).

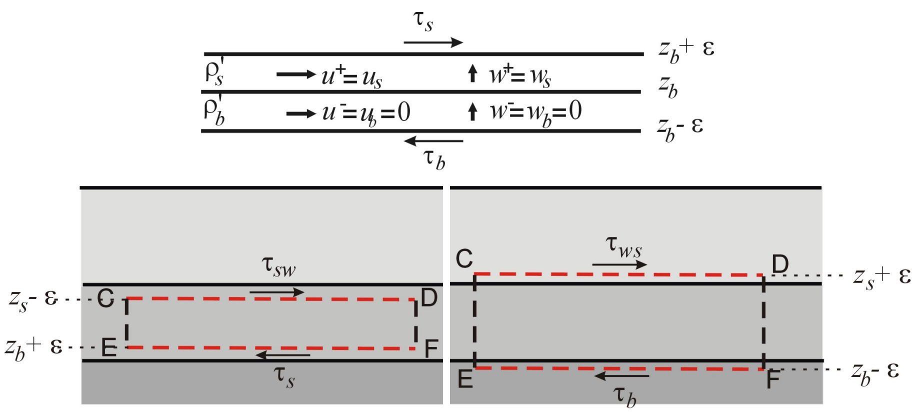

Figure 2.11. Interface z_b and transport layer control volume definition (mobile boundaries in red)

As it was exposed for the water control volume, the boundary CD will be positioned at z_s+ε in the following. Identically to the control volume boundary CD linked to the interface z_s, EF has to be slightly above (z_b + ε) or below (z_b - ε) the interface z_b and moves vertically at the rate $\partial z_b/\partial t$ in case of erosion or deposition. If the bottom limit (z_b - ε) is chosen, which is the case in the following, the external shear stress applied on the control surface EF is the shear stress τ_b. In the other case, it would have been τ_s, the resulting equations would have been identical.

Continuity equation on the water layer

The Lagrangian Eulerian conservation of the mass *m* writes:

$$\frac{Dm}{Dt} = \frac{\partial}{\partial t}\iiint_{\mathrm{CV}} \rho\, dV + \iint_{\mathrm{CS}} \rho\left(\mathbf{V}_r \,|\, d\mathbf{A}\right) = 0 \tag{2.40}$$

where CV is the considered control volume bounded by the control surfaces CS and $\mathbf{V}_r$ is the velocity relative to the boundary. If the interfaces (boundary surfaces) of the control volume do not move, $\mathbf{V}_\mathbf{r}$ is equal to the velocity of the fluid crossing the interfaces.

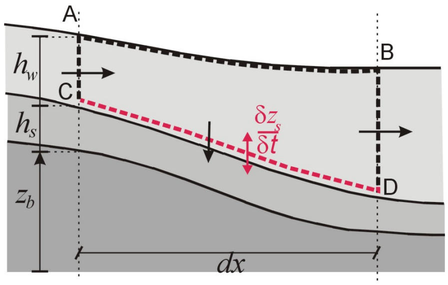

Figure 2.12. Water control volume (mobile boundaries in red)

The Lagrangian Eulerian conservation of the mass (2.40) is applied to the control volume ABCD (Fig. 2.12). The boundary CD, located at z_s+ε, is mobile. A mass flux is calculated through the vertical non-mobile interfaces AC and BD and through the mobile interface CD. Even if the water has no vertical component, the interface CD is moving ($\partial z_s/\partial t < 0$ in case of deposition, $\partial z_s/\partial t > 0$ in case of erosion), in such a way that a velocity relative to this boundary $\mathbf{V_r} = \partial z_s / \partial t$ has to be considered. The continuity equation of water phase reads

$$\rho_w \frac{\partial h_w}{\partial t} dx \underbrace{-\rho_w h_w u_w}_{\text{mass flux AC}} + \underbrace{\rho_w h_w u_w + \rho_w \frac{\partial h_w u_w}{\partial x} dx}_{\text{mass flux BD}} + \underbrace{\rho_w \frac{\partial z_s}{\partial t} dx}_{\text{mass flux CD}} = 0 \tag{2.41}$$

which is simplified to give the first equation of the system.

$$\frac{\partial h_w}{\partial t} + \frac{\partial h_w u_w}{\partial x} = -\frac{\partial z_s}{\partial t} = e_s \tag{2.42}$$

Continuity equation on the transport layer

The continuity equation on the sediment transport layer is obtained by applying (2.40) to the control volume CDEF (Fig. 2.13). An additional mass flux should now be taken into account at the mobile interface EF, located at z_b - ε.

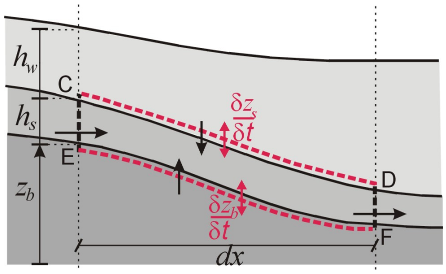

Figure 2.13. Transport layer control volume (mobile boundaries in red)

The sediments do not move vertically in the bed, but the interface EF is moving ($\partial z_b / \partial t < 0$ in case of erosion, $\partial z_b / \partial t > 0$ in case of deposition), in such a way that a velocity relative to this boundary is to be considered. Equation (2.40) reads

$$\rho_s'\frac{\partial h_s}{\partial t}dx\underbrace{-\rho_s' h_s u_s}_{\text{mass flux CE}}\underbrace{+\rho_s' h_s u_s+\rho_s'\frac{\partial h_s u_s}{\partial x}dx}_{\text{mass flux DF}}\underbrace{+\rho_b'\frac{\partial z_b}{\partial t}dx}_{\text{mass flux EF}}\underbrace{-\rho_w\frac{\partial z_s}{\partial t}dx}_{\text{mass flux CD}}=0 \tag{2.43}$$

$$\frac{\partial h_s}{\partial t}+\frac{\partial h_s u_s}{\partial x}=-\frac{\rho_b'}{\rho_s'}\frac{\partial z_b}{\partial t}+\frac{\rho_w}{\rho_s'}\frac{\partial z_s}{\partial t}=\frac{\rho_b'}{\rho_s'}e_b-\frac{\rho_w}{\rho_s'}e_s \tag{2.44}$$

The time variation of the mass in the control volume due to the displacement of the interfaces EF and CD can also be expressed as

$$\rho_s'\frac{\partial h_s}{\partial t}dx\underbrace{-\rho_s' h_s u_s}_{\text{mass flux CE}}\underbrace{+\rho_s' h_s u_s+\rho_s'\frac{\partial h_s u_s}{\partial x}dx}_{\text{mass flux DF}}\underbrace{+\rho_{s'}\left(\frac{\partial z_b}{\partial t}-\frac{\partial z_s}{\partial t}\right)dx}_{\text{mass flux EF+CD}}=0 \tag{2.45}$$

which leads to another expression of the sediment transport layer continuity equation (2.44)

$$\frac{\partial h_s}{\partial t}+\frac{\partial h_s u_s}{\partial x}=e_b-e_s \tag{2.46}$$

Both expressions (2.44) and (2.46) are equivalent, as, from (2.29):

$$\frac{\rho_b'}{\rho_s'}e_b-\frac{\rho_w}{\rho_s'}e_s=e_b-e_s \tag{2.47}$$

Momentum equation on the water layer

The Lagrangian Eulerian conservation of momentum in the x-direction may be expressed:

$$\sum \mathbf{F}_x=\frac{D\left(mu\right)}{Dt}=\frac{\partial}{\partial t}\iiint_{\mathrm{CV}}\rho\, u\, dV+\iint_{\mathrm{CS}}\rho u\left(\mathbf{V}_r\,|d\mathbf{A}\right) \tag{2.48}$$

where u is the x-component of the absolute velocity and $\mathbf{V}_r$ is the relative velocity of the fluid crossing the interface.

The momentum equation of the water phase is obtained by applying (2.48) on the control volume ABCD as defined in Figure 2.12. In (2.48), only the horizontal components of the forces are considered, as the sum of the vertical components is equal to zero (Fig. 2.14).

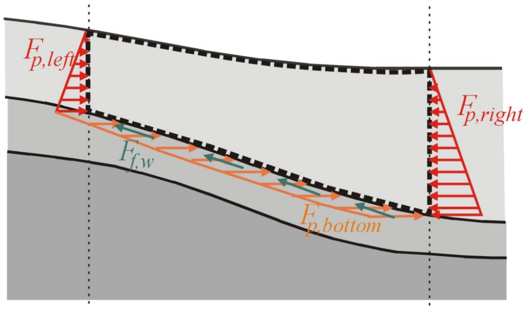

Figure 2.14. Forces applied on the water control volume

The shallow-water assumption implies hydrostatic distribution of pressure. The sum of the forces in the x-direction gives

$$\sum \mathbf{F}_x = F_{p,\,\text{left}} - F_{p,\,\text{right}} + F_{p,\,\text{bottom}} - F_{f,w} \tag{2.49}$$

where

$F_{p,left}$ is the pressure force applied on the left interface of the control volume.

$$F_{p,left} = \frac{1}{2}\rho_w g h_w^2 \tag{2.50}$$

$F_{p,right}$ is the pressure force applied on the right interface of the control volume.

$$F_{p,right} = F_{p,left} + \frac{\partial F_{p,left}}{\partial x}dx = \frac{1}{2}\rho_w g h_w^2 + \frac{1}{2}\rho_w g \frac{\partial h_w^2}{\partial x}dx \tag{2.51}$$

$F_{p,bottom}$ is the horizontal component of the pressure force applied on the bottom interface of the control volume. This force is calculated as the arithmetical average between the pressure at the left and right sides of the bottom interface multiplied by the vertical projection of the surface.

$$F_{p,bottom} = -\frac{1}{2}\left(\rho_w g h_w + \left(\rho_w g h_w + \frac{\partial \rho_w g h_w}{\partial x} dx\right)\right)\frac{\partial (z_b + h_s)}{\partial x} dx \tag{2.52}$$

As the second order terms are neglected, the expression can be simplified.

$$F_{p,bottom} = -\rho_w g h_w \frac{\partial (z_b + h_s)}{\partial x} dx \tag{2.53}$$

As CD is located above z_s in the water layer, $F_{f,w}$ is the horizontal component of the reaction due to the friction shear stress τ_{ws} applied by the water layer on the transport layer. If CD was located below z_s, the friction shear stress τ_{sw} would have been considered.

$$F_{f,w} = \tau_{ws}\sqrt{1 - \left(\frac{\partial (z_b + h_s)}{\partial x}\right)^2} dx \tag{2.54}$$

which is simplified (second-order terms are neglected)

$$F_{f,w} = \tau_{ws} dx \tag{2.55}$$

All these expressions are substituted in (2.49) and the resulting force is

$$\sum \vec{F} = -\frac{1}{2}\rho_w g \frac{\partial h_w^2}{\partial x} dx - \rho_w g h_w \frac{\partial (z_b + h_s)}{\partial x} dx - \tau_{ws} dx \tag{2.56}$$

The change in sediment concentration implies an exchange of momentum between the water and the transport layers (boundary CD). This exchange is characterised by the velocity of the fluid crossing the boundary. As the boundary CD is located in the water layer, the velocity in the x-direction is u_w. As exposed above (2.37), the velocity in the z-direction is $w_w = 0$, it induces the velocity relative to the interface CD is only due to the movement of this interface, which is characterised by the velocity $\partial z_s / \partial t = -e_s$. The water material derivative of the momentum (2.48) becomes

$$\frac{D(mu)}{Dt} = \rho_w \frac{\partial h_w u_w}{\partial t} dx \underbrace{- \rho_w\, h_w\, u_w^2}_{\text{mom flux AC}}$$

$$+ \underbrace{\rho_w h_w u_w^2 + \rho_w \frac{\partial h_w u_w^2}{\partial x} dx}_{\text{mom. flux BD}} + \underbrace{\rho_w u_w \frac{\partial z_s}{\partial t} dx}_{\text{mom. flux CD}} \qquad (2.57)$$

$$= \rho_w \frac{\partial h_w u_w}{\partial t} dx + \rho_w \frac{\partial h_w u_w^2}{\partial x} dx + \rho_w u_w \frac{\partial z_s}{\partial t} dx$$

Substituting (2.56) and (2.57) into (2.48), provides the momentum equation of the water phase

$$\frac{\partial h_w u_w}{\partial t} + \frac{\partial}{\partial x}\left(h_w u_w^2 + \frac{1}{2} g h_w^2 \right) + g h_w \frac{\partial (z_b + h_s)}{\partial x} = u_w e_s - \frac{\tau_{ws}}{\rho_w} \qquad (2.58)$$

If the boundary CD was set to $z_s - \varepsilon$ instead of $z_s + \varepsilon$, the external force $F_{f,w}$ (2.55) applied on CD would depend on τ_{sw} instead of τ_{ws}. Moreover, the x-velocity of the flow crossing CD would be u_s and the relative velocity would take into account the non-zero vertical velocity w_s in addition to the interface displacement e_s.

The momentum equation under these conditions becomes

$$\frac{\partial h_w u_w}{\partial t} + \frac{\partial}{\partial x}\left(h_w u_w^2 + \frac{1}{2} g h_w^2 \right) + g h_w \frac{\partial (z_b + h_s)}{\partial x} = \frac{\rho_s'}{\rho_w} u_s (w_s + e_s) - \frac{\tau_{sw}}{\rho_w} \qquad (2.59)$$

If the expression of w_s (2.32) and τ_{sw} (2.39) are substituted, it reduces to the momentum equation (2.58).

Momentum equation on the transport layer

The momentum equation (2.48) is now applied on the control volume CDEF defined in Figure 2.13. The forces in the *x*-direction are defined in Figure 2.15.

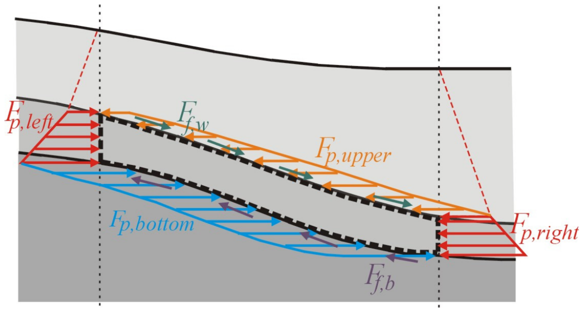

Figure 2.15. Forces applied on the transport layer control volume

The sum of the forces in the *x*-direction gives

$$\sum \mathbf{F}_x = F_{p,\,\text{left}} - F_{p,\,\text{right}} - F_{p,\,\text{upper}} + F_{p,\,\text{bottom}} + F_{f,w} - F_{f,b} \tag{2.60}$$

where

$F_{p,left}$ is the pressure force applied on the left interface of the control volume.

$$F_{p,left} = \frac{1}{2}\rho_s' g h_s^2 + \rho_w g h_w h_s \tag{2.61}$$

$F_{p,right}$ is the pressure force applied on the right interface of the control volume.

$$\begin{aligned} F_{p,right} &= F_{p,left} + \frac{\partial\left(\frac{1}{2}\rho_s' g h_s^2 + \rho_w g h_w h_s\right)}{\partial x} dx \\ &= F_{p,left} + \frac{1}{2}\rho_s' g \frac{\partial h_s^2}{\partial x} dx + \rho_w g h_w \frac{\partial h_s}{\partial x} dx + \rho_w g h_s \frac{\partial h_w}{\partial x} dx \end{aligned} \tag{2.62}$$

$F_{p,upper}$ is the horizontal component of the pressure force applied by the water layer on the sediment transport layer (second order terms are neglected).

$$F_{p,upper} = -\rho_w g h_w \frac{\partial(z_b + h_s)}{\partial x} dx \tag{2.63}$$

$F_{p,bottom}$ is the horizontal component of the pressure force applied on the bottom interface of the control volume (second order terms are neglected).

$$F_{p,bottom} = (\rho_w g h_w + \rho_s' g h_s)\frac{\partial z_b}{\partial x} dx \tag{2.64}$$

$F_{f,w}$ is the horizontal component of the frictional force between the water layer and the transport layer (second order terms are neglected).

$$F_{f,w} = \tau_{ws} dx \tag{2.65}$$

$F_{f,b}$ is the horizontal component expressing the resistance by the fixed bed to the transport layer movement (second order terms are neglected).

$$F_{f,b} = \tau_b dx \tag{2.66}$$

All these expressions are substituted in (2.60) and the resulting force is

$$\begin{aligned}\sum \mathbf{F}_x = &-\frac{1}{2}\rho_s g h_s \frac{\partial h_s^2}{\partial x} dx - \rho_w g h_s \frac{\partial h_w}{\partial x} dx \\ &- \rho_s' g h_s \frac{\partial z_b}{\partial x} dx + \tau_{ws} dx - \tau_b dx\end{aligned} \tag{2.67}$$

In addition to the momentum fluxes through the lateral interfaces CE and DF, the momentum exchange at the interface between the water and the transport layers CD has to be introduced in equation (2.48), the momentum flux through the mobile boundary EF being equal to zero. Indeed, the motion of the control surface EF, due to erosion or deposition, induces a mass flux through this boundary (as taken into account in 2.43), but no momentum flux as the velocity u_b related to the mass crossing this boundary is equal to zero (velocity in the bed). The material derivative of the momentum of the sediment transport layer (2.48) becomes in case of erosion

$$\begin{aligned}\frac{D(mu)}{Dt} &= \rho_s'\frac{\partial h_s u_s}{\partial t}dx \underbrace{-\rho_s' h_s u_s^2}_{\text{mom. flux CE}} \\ &\quad \underbrace{+\rho_s' h_s u_s^2 + \rho_s'\frac{\partial h_s u_s^2}{\partial x}dx}_{\text{mom. flux DF}} \underbrace{-\rho_w u_w \frac{\partial z_s}{\partial t}dx}_{\text{mom. flux CD}} \qquad (2.68) \\ &= \rho_s'\frac{\partial h_s u_s}{\partial t}dx + \rho_s'\frac{\partial h_s u_s^2}{\partial x}dx - \rho_w u_w \frac{\partial z_s}{\partial t}dx\end{aligned}$$

Substituting (2.67) and (2.68) into (2.48), provides the momentum equation of the mixture phase

$$\begin{aligned}&\frac{\partial h_s u_s}{\partial t} + \frac{\partial}{\partial x}\left(h_s u_s^2 + \frac{1}{2}g h_s^2\right) + g h_s \frac{\partial}{\partial x}\left(z_b + \frac{\rho_w}{\rho_s'}h_w\right) \\ &\qquad = -\frac{\rho_w}{\rho_{s'}}u_w e_s + \frac{\tau_{ws}}{\rho_s'} - \frac{\tau_b}{\rho_s'}\end{aligned} \qquad (2.69)$$

If the control volume boundary was chosen to correspond to the upper limit ($z_b + \varepsilon$) (Fig. 2.11) the shear stress τ_s would be the external shear stress applied on the control surface EF (τ_b would be replaced by τ_s in 2.67). In this case, if erosion or deposition occurred, in addition to the mass flux crossing the mobile boundary EF, an exchange of momentum should be taken into account as the velocity of the mass crossing the interface would be u_s. The resulting momentum equation would be the same.

Shear stresses

The shear stress applied by water on the transport layer τ_{ws} and the shear stress acting on the fixed bed τ_s are assumed to follow a Chézy-like friction law:

$$\tau_{ws} = \rho_w C_{f,w} |u_w - u_s| \left(u_w - u_s\right) \tag{2.70}$$

$$\tau_s = \rho_s' C_{f,s} |u_s| \, u_s \tag{2.71}$$

where $C_{f,w}$ and $C_{f,s}$ are water and sediment friction coefficients. In order to simplify notations, in the following, when no confusion will be possible, τ_{ws} will be named τ_w. No relation is available for τ_{sw}, which is unimportant since all may be expressed as a function of τ_{ws} only. A Mohr–Coulomb relation, expresses the shear stress resisting to the flow of the sediment transport layer, applied by the fixed bed.

$$\tau_b = \tau_{crit} + tg\varphi(\rho_s' - \rho_w) g h_s \tag{2.72}$$

where τ_{crit} is the threshold value of τ_s allowing erosion and φ is the internal friction angle of the soil. This angle is assumed to be the same when sediments have been remoulded or not. The characteristics of the sediments only appear through ρ_s, τ_{crit}, φ, $C_{f,s}$ and $C_{f,w}$. The mean grain diameter does not explicitly appear, but it is present through τ_{crit}, $C_{f,s}$, and $C_{f,w}$, whose calibration values depend on the grain diameter. In the present thesis, only non-cohesive sediments are considered, the sand used in the experiments has a characteristic grain diameter of 1.65 mm. The model was previously applied to simulate experiments with extruded PVC pellets slightly cylindrical in shape having an equivalent diameter of 3.9 mm. For other grain diameters, the model remains valid if the diameter and the flow conditions lead to a bed load sediment transport mechanism. The range of application o this two-layer model can be extended to debris flow. In this case, the closure relations (shear stresses) should be modified to take into account rheology (Peng, 2004; Chen et al, 2007).

Summary

The previous demonstrations leads to a five-equation set (2.42), (2.46), (2.58), (2.69) and the definition of the erosion rate (2.35).

$$\frac{\partial h_w}{\partial t}+\frac{\partial h_w u_w}{\partial x}=e_s \tag{2.73}$$

$$\frac{\partial h_s}{\partial t}+\frac{\partial h_s u_s}{\partial x}=e_b-e_s \tag{2.74}$$

$$\frac{\partial z_b}{\partial t}=-e_b \tag{2.75}$$

$$\frac{\partial h_w u_w}{\partial t}+\frac{\partial}{\partial x}\left(h_w u_w^2+\frac{1}{2}gh_w^2\right)+gh_w\frac{\partial(z_b+h_s)}{\partial x}=u_w e_s-\frac{\tau_{ws}}{\rho_w} \tag{2.76}$$

$$\frac{\partial h_s u_s}{\partial t}+\frac{\partial}{\partial x}\left(h_s u_s^2+\frac{1}{2}gh_s^2\right)+gh_s\frac{\partial}{\partial x}\left(z_b+\frac{\rho_w}{\rho_s'}h_w\right)=-\frac{\rho_w}{\rho_{s'}}u_w e_s+\frac{\tau_{ws}}{\rho_s'}-\frac{\tau_b}{\rho_s'} \tag{2.77}$$

where e_b and e_s depend on the shear stresses on both sides of the respective interface z_b (2.35) and z_s (2.39) and are related to each other by (2.29)

$$e_s=\frac{\tau_{ws}-\tau_{sw}}{\rho_w(u_w-u_s)}=-\frac{\rho_b'-\rho_s'}{\rho_s'-\rho_w}e_b=-\frac{C_b-C_s}{C_s}e_b \tag{2.78}$$

$$e_b=\frac{\tau_s-\tau_b}{\rho_b' u_s} \tag{2.79}$$

where the shear stresses are (2.70), (2.71) and (2.72)

$$\tau_{ws}=\rho_w C_{f,w}\left|u_w-u_s\right|\left(u_w-u_s\right) \tag{2.80}$$

$$\tau_s=\rho_s' C_{f,s}\left|u_s\right|u_s \tag{2.81}$$

$$\tau_b = \tau_{crit} + tg\varphi(\rho_s{}' - \rho_w) g h_s \tag{2.82}$$

The system of equations (2.73), (2.74), (2.75), (2.76) and (2.77) can be rewritten under a vector formulation.

$$\frac{\partial \mathbf{U}}{\partial t} + \frac{\partial \mathbf{F}(\mathbf{U})}{\partial x} + \mathbf{H}'(\mathbf{U}) \frac{\partial \mathbf{U}}{\partial x} = \mathbf{S}(\mathbf{U}) \tag{2.83}$$

with $$\mathbf{U} = \begin{pmatrix} h_w \\ h_s \\ z_b \\ h_w u_w \\ h_s u_s \end{pmatrix} = \begin{pmatrix} h_w \\ h_s \\ z_b \\ q_w \\ q_s \end{pmatrix} \qquad \mathbf{F}(\mathbf{U}) = \begin{pmatrix} h_w u_w \\ h_s u_s \\ 0 \\ h_w u_w^2 + \frac{1}{2} g h_w^2 \\ h_s u_s^2 + \frac{1}{2} g h_s^2 \end{pmatrix} \tag{2.84}$$

$$\mathbf{H}'(\mathbf{U}) = \begin{pmatrix} 0 & 0 & 0 & 0 & 0 \\ 0 & 0 & 0 & 0 & 0 \\ 0 & 0 & 0 & 0 & 0 \\ 0 & g h_w & g h_w & 0 & 0 \\ \frac{\rho_w}{\rho_s{}'} g h_s & 0 & g h_s & 0 & 0 \end{pmatrix}$$

$$\mathbf{S}(\mathbf{U}) = \begin{pmatrix} e_s \\ e_b - e_s \\ -e_b \\ u_w e_s - \dfrac{\tau_{ws}}{\rho_w} \\ -\dfrac{\rho_w}{\rho_s{}'} u_w e_s + \dfrac{\tau_{ws} - \tau_b}{\rho_s{}'} \end{pmatrix} \tag{2.85}$$

or

$$\frac{\partial \mathbf{U}}{\partial t} + \frac{\partial \mathbf{F}(\mathbf{U})}{\partial x} + \mathbf{H}(\mathbf{U}) \frac{\partial \mathbf{G}(\mathbf{U})}{\partial x} = \mathbf{S}(\mathbf{U}) \tag{2.86}$$

with $$\mathbf{H}(\mathbf{U})=\begin{pmatrix}0\\0\\0\\gh_w\\gh_s\end{pmatrix} \qquad \mathbf{G}(\mathbf{U})=\begin{pmatrix}0\\0\\0\\z_b+h_s\\z_b+\dfrac{\rho_w}{\rho_s'}h_w\end{pmatrix} \tag{2.87}$$

2.1.2.2. Two-velocity one-concentration model

The two-layer model presented by Capart and Young (2002) and exposed in more detail in the case of mud-flow by Chen et al (2007) can be deduced from equations (2.73), (2.74), (2.75), (2.76) and (2.77) obtained previously. The main variables and assumptions are identical to those concerning the two-velocity, two-concentration model described above, except concerning the sediment concentration of the transport layer. In the present model, the sediment concentration in the transport layer is assumed to be identical to the one in the bed $C = C_s = C_b$.

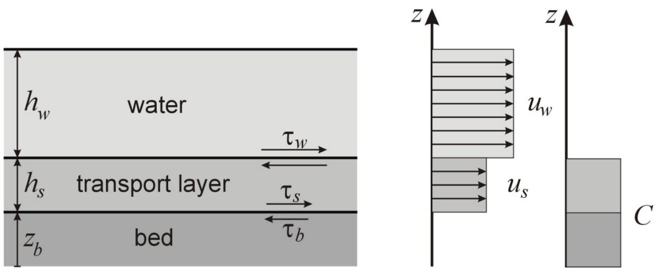

Figure 2.16. Two-velocity one-concentration model

The decrease of concentration due to the sediment mobilisation is neglected. The volumetric mass in the sediment transport layer and in the bed are then identical $\rho_s' = \rho_b = (1-C)\rho_w + C\rho_s$. As there is no change in concentration when sediments move between the bed and the transport layer, from (2.29), it can be deduced that the interface z_s does not move ($e_s = 0$) during erosion or deposition process. There is neither mass nor momentum exchange at this interface. Then, (2.39) leads to consider there is no difference between the shear stress on each side of this interface due to friction between the two layers ($\tau_w = \tau_{ws} = \tau_{sw}$). If the evolution rate e_s is set to zero in the system of equations (2.73), (2.74), (2.75), (2.76) and (2.77), it becomes

$$\frac{\partial h_w}{\partial t} + \frac{\partial h_w u_w}{\partial x} = 0 \tag{2.88}$$

$$\frac{\partial h_s}{\partial t} + \frac{\partial h_s u_s}{\partial x} = e_b \tag{2.89}$$

$$\frac{\partial z_b}{\partial t} = -e_b \tag{2.90}$$

$$\frac{\partial h_w u_w}{\partial t} + \frac{\partial}{\partial x}\left(h_w u_w^2 + \frac{1}{2} g h_w^2 \right) + g h_w \frac{\partial (z_b + h_s)}{\partial x} = -\frac{\tau_w}{\rho_w} \tag{2.91}$$

$$\frac{\partial h_s u_s}{\partial t} + \frac{\partial}{\partial x}\left(h_s u_s^2 + \frac{1}{2} g h_s^2 \right) + g h_s \frac{\partial}{\partial x}\left(z_b + \frac{\rho_w}{\rho_s'} h_s \right) = \frac{\tau_w}{\rho_s'} - \frac{\tau_b}{\rho_s'} \tag{2.92}$$

where the erosion rate e_b (2.35) and the shear stresses τ_w (2.80), τ_s (2.81) and τ_b (2.82) keep the same definition. Only the source terms are affected by the assumption concerning the concentration in sediment of the transport layer.

The system of equations (2.88), (2.89), (2.90), (2.91) and (2.92) can be rewritten under the vector formulation (2.83), where only the source terms **S**(**U**) are modified.

$$\mathbf{S}(\mathbf{U}) = \begin{pmatrix} 0 \\ e_b \\ -e_b \\ -\dfrac{\tau_w}{\rho_w} \\ \dfrac{\tau_w - \tau_b}{\rho_s'} \end{pmatrix} = \begin{pmatrix} 0 \\ \dfrac{\tau_s - \tau_b}{\rho_s' u_s} \\ -\dfrac{\tau_s - \tau_b}{\rho_s' u_s} \\ -\dfrac{\tau_w}{\rho_w} \\ \dfrac{\tau_w - \tau_b}{\rho_s'} \end{pmatrix} \tag{2.93}$$

2.1.2.3. *Model with specific assumption on the velocity in the transport layer*

Constant velocity ratio model

As demonstrated previously by other authors (for example Lawrence, 1990 and Spinewine, 2005), the loss of hyperbolicity of the two-velocity model, for a range of flow conditions, will be underlined in section 2.2.4. An adaptation of the above model is thus proposed in order to maintain a hyperbolic problem. In each of the applications treated in the present thesis, it was noticed than the ratio between the velocity in the sediment transport and in the water layer $\alpha = u_s / u_w$ is almost constant. The proposal consists in imposing this velocity ratio from the beginning of the calculation. The calibration process of this fixed ratio will be exposed in chapter 6. The relevance of this proposal will be studied all along the thesis. The stratified flow is pictured on Figure 2.17.

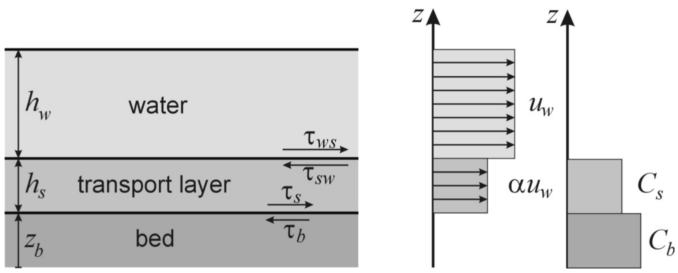

Figure 2.17. Constant velocity ratio model

All the assumptions are identical to the ones developed in the above sections. The only change concerns the velocity in the sediment transport layer, which is not a main unknown anymore, it is assumed to be directly proportional, with a constant ratio α, to the velocity in the water layer.

$$u_s = \alpha u_w \tag{2.94}$$

In the particular case of pure hydrodynamic flow, without sediment transport ($h_s = 0$), the velocity ratio has to be set to zero.

The mass conservation on the water layer remains identical to (2.73)

$$\frac{\partial h_w}{\partial t} + \frac{\partial h_w u_w}{\partial x} = e_s \tag{2.95}$$

while from (2.94), the mass conservation on the sediment layer (2.74) becomes

$$\frac{\partial h_s}{\partial t} + \alpha \frac{\partial h_s u_w}{\partial x} = e_b - e_s \tag{2.96}$$

The displacement of the interface z_b with time remains identical to (2.75)

$$\frac{\partial z_b}{\partial t} = -e_b \tag{2.97}$$

The momentum equation on the water layer (2.76) multiplied by ρ_w is added to the momentum equation on the sediment transport layer (2.77), in which the expression of u_s (2.94) is substituted, multiplied by ρ_s'.

$$\begin{aligned}
&\frac{\partial}{\partial t}\left(\rho_w h_w u_w + \alpha\rho_s' h_s u_w\right) \\
&+ \frac{\partial}{\partial x}\left(\rho_w h_w u_w^2 + \frac{1}{2}\rho_w g h_w^2 + \alpha^2\rho_s' h_s u_s^2 + \frac{1}{2}\rho_s' g h_s^2\right) \\
&+ \rho_w g h_w \frac{\partial(z_b + h_s)}{\partial x} + \rho_s' g h_s \frac{\partial}{\partial x}\left(z_b + \frac{\rho_w}{\rho_s'} h_w\right) = -\tau_b
\end{aligned} \tag{2.98}$$

The expression of u_s (2.94) has to be substituted in the erosion rate definition (2.35) and in the expression of the shear stress applied on the fixed bed τ_s

$$e_b = \frac{\tau_s - \tau_b}{\alpha\rho_b u_w} \qquad\qquad \tau_s = \alpha^2\rho_s' C_{f,s}\left|u_w\right| u_w \tag{2.99}$$

The expressions of e_s (2.29) and the shear stress resisting to the flow τ_b (2.82) do not change.

The system of equations (2.95), (2.96), (2.97) and (2.98) can be rewritten

$$\frac{\partial \mathbf{U}}{\partial t}+\frac{\partial \mathbf{F}(\mathbf{U})}{\partial x}+\mathbf{H}'(\mathbf{U})\frac{\partial \mathbf{U}}{\partial x}=\mathbf{S}(\mathbf{U}) \tag{2.100}$$

with
$$\mathbf{U}=\begin{pmatrix} h_w \\ h_s \\ z_b \\ (\rho_w h_w+\alpha\rho_s' h_s)u_w \end{pmatrix}$$

$$\mathbf{F}(\mathbf{U})=\begin{pmatrix} h_w u_w \\ \alpha h_s u_w \\ 0 \\ \rho_w h_w u_w^2+\frac{1}{2}\rho_w g h_w^2+\alpha^2\rho_s' h_s u_s^2+\frac{1}{2}\rho_s' g h_s^2 \end{pmatrix} \tag{2.101}$$

$$\mathbf{H}'(\mathbf{U})=\begin{pmatrix} 0 & 0 & 0 & 0 \\ 0 & 0 & 0 & 0 \\ 0 & 0 & 0 & 0 \\ \rho_w g h_s & \rho_w g h_w & \rho_w g h_w+\rho_s' g h_s & 0 \end{pmatrix} \quad \mathbf{S}(\mathbf{U})=\begin{pmatrix} e_s \\ e_b-e_s \\ -e_b \\ -\tau_b \end{pmatrix} \tag{2.102}$$

If the derivatives are developed and the continuity relations (2.95) and (2.96) are substituted, the momentum equation (2.98) can write

$$\begin{aligned}\frac{\partial u_w}{\partial t}&+\frac{\rho_w h_w+\alpha^2\rho_s' h_s}{\rho_w h_w+\alpha\rho_s' h_s}u_w\frac{\partial u_w}{\partial x}+\frac{\rho_w g h_w+\rho_w g h_s}{\rho_w h_w+\alpha\rho_s' h_s}\frac{\partial h_w}{\partial x}\\ &+\frac{\rho_w g h_w+\rho_s' g h_s}{\rho_w h_w+\alpha\rho_s' h_s}\frac{\partial h_s}{\partial x}+\frac{\rho_w g h_w+\rho_s' g h_s}{\rho_w h_w+\alpha\rho_s' h_s}\frac{\partial z_b}{\partial x}\\ &=\frac{-\tau_b-\rho_w u_w e_s-\alpha\rho_s' u_w(e_b-e_s)}{\rho_w h_w+\alpha\rho_s' h_s}\end{aligned} \tag{2.103}$$

The system of equations (2.95), (2.96), (2.97) and (2.103) can be rewritten under a vector formulation (2.100)

with $$\mathbf{U} = \begin{pmatrix} h_w \\ h_s \\ z_b \\ u_w \end{pmatrix} \qquad \mathbf{F}(\mathbf{U}) = \begin{pmatrix} h_w u_w \\ \alpha h_s u_w \\ 0 \\ 0 \end{pmatrix} \tag{2.104}$$

$$\mathbf{H}'(\mathbf{U}) = \begin{pmatrix} 0 & 0 & 0 & 0 \\ 0 & 0 & 0 & 0 \\ 0 & 0 & 0 & 0 \\ \xi & \dfrac{\rho_w g h_w + \rho_s' g h_s}{\rho_w h_w + \alpha\rho_s' h_s} & \xi & \dfrac{\rho_w h_w + \alpha^2 \rho_s' h_s}{\rho_w h_w + \alpha\rho_s' h_s} u_w \end{pmatrix}$$

where $$\xi = \frac{\rho_w g h_w + \rho_w g h_s}{\rho_w h_w + \alpha\rho_s' h_s}$$

$$\mathbf{S}(\mathbf{U}) = \begin{pmatrix} e_s \\ e_b - e_s \\ -e_b \\ \dfrac{-\tau_b - \rho_w u_w e_s - \alpha\rho_s' u_w (e_b - e_s)}{\rho_w h_w + \alpha\rho_s' h_s} \end{pmatrix} \tag{2.105}$$

One-velocity one-concentration model

The simplified model considering the same velocity in the water and in the sediment transport (Capart 2000) has been demonstrated by Fraccarollo and Capart (2002) and can be easily deduced from the equations (2.88), (2.89), (2.90), (2.91) and (2.92) obtained previously. The assumptions are identical to those concerning the model described above, except the velocities are the same in the water and the transport layer. The main unknowns are the thickness of the transport layer h_s, the total transport depth $h_m = h_w + h_s$ the common velocity $u_m = u_w = u_s$ and the level z_b of the interface between the bed and the transport layer (Fig.2.18).

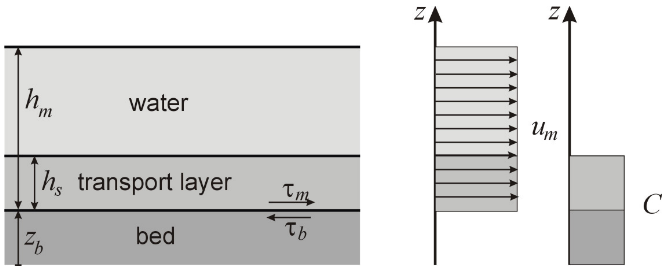

Figure 2.18. One-velocity one-concentration model

As the velocity of water and sediments in the transport layer are identical, there is no imbalance of shear stress between the water and the transport layer. If the velocities in the water layer and in the transport layer are the same in the five-equation system (2.73-2.77), it reduces to four equations.

The first equation is obtained by addition of the two equations of continuity (2.88) and (2.89)

$$\frac{\partial h_m}{\partial t} + \frac{\partial h_m u_m}{\partial x} = e_b \tag{2.106}$$

The second one is equivalent to equation (2.89)

$$\frac{\partial h_s}{\partial t} + \frac{\partial h_s u_m}{\partial x} = e_b \tag{2.107}$$

The third one is the definition of the erosion rate e_b

$$\frac{\partial z_b}{\partial t} = -e_b \tag{2.108}$$

The last one is obtained by adding (2.91) to (2.92) multiplied by $\rho_s'/\rho_w = 1 + r$, subtracting (2.88) and (2.89), the latter multiplied by $\rho_s'/\rho_w\, u_m = (1+r)\, u_m$, and dividing the so-obtained sum by $(h_m + r\,h_s)$.

$$\frac{\partial u_m}{\partial t} + \frac{\partial}{\partial x}\left(\frac{u_m^2}{2}\right) + \frac{g}{2}\,\frac{1}{h_m + r\,h_s}\,\frac{\partial}{\partial x}\left(h_m^2 + r\,h_s^2\right) + g\,\frac{\partial z_b}{\partial x} = -\frac{\tau_m}{\rho_w\,(h_m + r\,h_s)} \tag{2.109}$$

where $r = C\left[\left(\rho_s - \rho_w\right)/\rho_w\right]$ is the correction factor accounting for the additional mass in the sediment layer compared to the water layer ($\rho_s'/\rho_w = 1 + r$).

As demonstrated in the previous section, the erosion rate defined as the velocity motion of the interface z_b, is depending on the difference between the two shear stresses acting on this interface.

$$e_b = \frac{\tau_m - \tau_b}{\rho_w (1+r) u_m} \tag{2.110}$$

The shear stress applied on the fixed bed τ_m is assumed to follow a Chézy friction law.

$$\tau_m = \rho_s' C_{fm} \left| u_m \right| u_m \tag{2.111}$$

where $C_{f,m}$ is the global friction coefficient.

The shear stress resisting to the flow in the fixed bed has a Mohr–Coulomb expression.

$$\tau_b = \tau_{crit} + tg\varphi(\rho_s' - \rho_w) g\, h_s \tag{2.112}$$

The system of equations (2.106), (2.107), (2.108) and (2.109) can be rewritten under a vector formulation

$$\frac{\partial \mathbf{U}}{\partial t} + \frac{\partial \mathbf{F}(\mathbf{U})}{\partial x} + \mathbf{H}'(\mathbf{U}) \frac{\partial \mathbf{U}}{\partial x} = \mathbf{S}(\mathbf{U}) \tag{2.113}$$

with $$\mathbf{U} = \begin{pmatrix} h_m \\ h_s \\ z_b \\ u_m \end{pmatrix} \qquad \mathbf{F}(\mathbf{U}) = \begin{pmatrix} h_m u_m \\ h_s u_m \\ 0 \\ \frac{1}{2} u_m^2 \end{pmatrix} \tag{2.114}$$

$$\mathbf{H}'(\mathbf{U}) = \begin{pmatrix} 0 & 0 & 0 & 0 \\ 0 & 0 & 0 & 0 \\ 0 & 0 & 0 & 0 \\ \dfrac{g\,h_m}{h_m + r\,h_s} & \dfrac{g\,r\,h_s}{h_m + r\,h_s} & g & 0 \end{pmatrix} \qquad \mathbf{S}(\mathbf{U}) = \begin{pmatrix} e_b \\ e_b \\ -e_b \\ -\dfrac{\tau_m}{\rho_w\,(h_m + r\,h_s)} \end{pmatrix} \tag{2.115}$$

or

$$\frac{\partial \mathbf{U}}{\partial t} + \frac{\partial \mathbf{F}(\mathbf{U})}{\partial x} + \mathbf{H}(\mathbf{U})\,\frac{\partial \mathbf{G}(\mathbf{U})}{\partial x} = \mathbf{S}(\mathbf{U}) \tag{2.116}$$

with $$\mathbf{H}(\mathbf{U}) = \begin{pmatrix} 0 \\ 0 \\ 0 \\ g(h_m + rh_s) \end{pmatrix} \qquad \mathbf{G}(\mathbf{U}) = \begin{pmatrix} 0 \\ 0 \\ 0 \\ z_b \end{pmatrix} \tag{2.117}$$

2.2. Eigenstructure analysis

Each set of equations proposed above to model shallow flows are supposed to be hyperbolic. It means that the equations are physically based on the propagation of information. The mathematical condition to qualify a system of equations to be hyperbolic is the eigenvalues, deduced from the Jacobian matrix of the system, have to be real. These eigenvalues represent the celerity of information, which is moving along characteristics curves in the plane (x, t), as detailed in Abbott (1979). Figure 2.19 illustrates the domain of influence of a perturbation and the domain of dependence of a situation, depending on the characteristic curves. The computation of the characteristics is rather simple in pure hydrodynamics, where the well-known Saint-Venant equations prevail. One of the possible ways to calculate the characteristics and the associated compatibility equations is an eigenvalue analysis of the Jacobian matrix of the system.

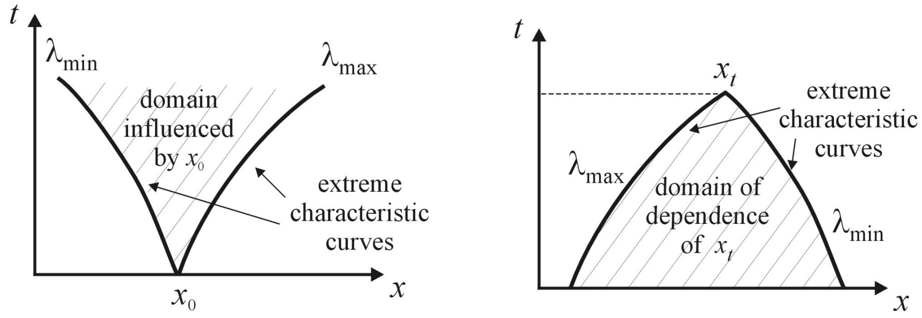

Figure 2.19. Influenced and dependent domain

Such an approach offers the ability to be extended, with an analytical solution, to the two-layer geomorphic equations in the simplified case where the velocity in both the water and the transport layers are explicitly linked. If those velocities are independent and in the case of the three-equation Saint-Venant – Exner model, this extension is also possible, but only by numerical approach.

2.2.1. Eigenvalue analysis in pure hydrodynamic case

To exemplify the eigenvalue strategy in a simple case, it is applied to the pure hydrodynamic case described by the Saint-Venant equations

$$\frac{\partial \mathbf{U}}{\partial t} + \frac{\partial \mathbf{F}(\mathbf{U})}{\partial x} = \frac{\partial \mathbf{U}}{\partial t} + \mathbf{A}\,\frac{\partial \mathbf{U}}{\partial x} = \mathbf{S}(\mathbf{U}) \tag{2.118}$$

where $\mathbf{U} = \begin{pmatrix} h \\ hu \end{pmatrix} = \begin{pmatrix} h \\ q \end{pmatrix} \qquad \mathbf{F}(\mathbf{U}) = \begin{pmatrix} hu \\ hu^2 + \frac{1}{2} gh^2 \end{pmatrix} \qquad \mathbf{S}(\mathbf{U}) = \begin{pmatrix} 0 \\ -\dfrac{\tau}{\rho} \end{pmatrix}$ (2.119)

and **A** is the Jacobian matrix of the system defined as

$$\mathbf{A} = \frac{\partial \mathbf{F}(\mathbf{U})}{\partial \mathbf{U}} = \begin{pmatrix} 0 & 1 \\ c^2 - u^2 & 2u \end{pmatrix} \quad \text{with} \quad c = \sqrt{gh} \tag{2.120}$$

The roots of equation

$$\left| \mathbf{A} - \lambda \mathbf{I} \right| = 0 \tag{2.121}$$

are the two eigenvalues λ_i of the Jacobian matrix **A,** corresponding to the celerities *dx*/*dt* of the two characteristics, the sign of them depending on the Froude number *u*/*c*.

$$\lambda_1 = u + c \qquad \lambda_2 = u - c \tag{2.122}$$

The left eigenvector $\mathbf{L}_i$ corresponding to the eigenvalue λ_i is defined by the expression

$$\mathbf{L}_i^{\mathrm{T}}\mathbf{A} = \lambda_i \mathbf{L}_i^{\mathrm{T}} \tag{2.123}$$

Defining the matrix **L**, whose line *i* is the left eigenvectors $\mathbf{L}_i$, and the diagonal matrix **D** containing the eigenvalues λ_i:

$$\mathbf{L} = \begin{pmatrix} \mathbf{L}_1^{\mathrm{T}} \\ \hdashline \mathbf{L}_2^{\mathrm{T}} \end{pmatrix} = \begin{pmatrix} l_{11} & l_{12} \\ l_{21} & l_{22} \end{pmatrix} = \begin{pmatrix} c-u & 1 \\ u+c & -1 \end{pmatrix}$$

$$\mathbf{D} = \begin{pmatrix} \lambda_1 & 0 \\ 0 & \lambda_2 \end{pmatrix} = \begin{pmatrix} u+c & 0 \\ 0 & u-c \end{pmatrix} \tag{2.124 a-b}$$

Equation (2.123) may be generalised in the form

$$\mathbf{L}\,\mathbf{A} = \mathbf{D}\,\mathbf{L} \tag{2.125}$$

Multiplying (2.118) by **L**, using (2.125) and neglecting the source terms gives

$$\mathbf{L}\frac{\partial}{\partial t}\begin{pmatrix} h \\ q \end{pmatrix} + \mathbf{L}\,\mathbf{A}\frac{\partial}{\partial x}\begin{pmatrix} h \\ q \end{pmatrix} = \mathbf{L}\frac{\partial}{\partial t}\begin{pmatrix} h \\ q \end{pmatrix} + \mathbf{D}\,\mathbf{L}\frac{\partial}{\partial x}\begin{pmatrix} h \\ q \end{pmatrix} = 0 \tag{2.126}$$

whose line *i* reads

$$\begin{aligned} & l_{i1}\frac{\partial h}{\partial t} + l_{i2}\frac{\partial q}{\partial t} + \lambda_i l_{i1}\frac{\partial h}{\partial x} + \lambda_i l_{i2}\frac{\partial q}{\partial x} \\ & \qquad = l_{i1}\left(\frac{\partial h}{\partial t} + \lambda_i\frac{\partial h}{\partial x}\right) + l_{i2}\left(\frac{\partial q}{\partial t} + \lambda_i\frac{\partial q}{\partial x}\right) = 0 \end{aligned} \tag{2.127}$$

Using the property linking partial and total derivatives: $d/dt = \partial/\partial t + (dx/dt)\,\partial/\partial x$ and considering that $\lambda_i = (dx/dt)_i$, (2.127) may be re-written

$$l_{i1}\left(\frac{dh}{dt}\right)_i + l_{i2}\left(\frac{dq}{dt}\right)_i = 0 \tag{2.128}$$

yielding the well-known compatibility relations

$$\left(\frac{dq}{dt}\right) + (-u + c)\left(\frac{dh}{dt}\right) = 0 \text{ along characteristic } \lambda_1 \tag{2.129a}$$

$$\left(\frac{dq}{dt}\right) + (-u - c)\left(\frac{dh}{dt}\right) = 0 \text{ along characteristic } \lambda_2 \tag{2.129b}$$

The compatibility relations illustrate the fact that the information propagating along one characteristic curve concerns a combination of the different variables and not only one variable. It is false to imagine that one characteristic is linked to the water depth h and the other to the discharge q, both are linked to both variables h and q. The left eigenvectors components appearing in the compatibility relations (2.129) give the part of information related to each variable.

It is possible to generalise the eigenstructure analysis to a system of n equations

$$\frac{\partial \mathbf{U}}{\partial t} + \mathbf{A}(\mathbf{U})\,\frac{\partial \mathbf{U}}{\partial x} = \mathbf{S}(\mathbf{U}) \tag{2.130}$$

The compatibility equation corresponding to the characteristic λ_i can be written

$$l_{i1}\left(\frac{d\mathbf{U}_1}{dt}\right)_{\lambda_i} + l_{i2}\left(\frac{d\mathbf{U}_2}{dt}\right)_{\lambda_i} + \ldots + l_{in}\left(\frac{d\mathbf{U}_n}{dt}\right)_{\lambda_i} = 0 \tag{2.131}$$

where $\mathbf{U}_j$ is the j-th component of the unknown vector $\mathbf{U}$, and l_{ij} the j-th component of the i-th left eigenvector $\mathbf{L}_i$.

2.2.2. Saint-Venant – Exner

Vreugdenhil and de Vries (1967) proposed the first eigenvalue analysis of the Saint-Venant – Exner equations (see also Jansen et al. 1979). Then the behaviour of these equations in case of near-critical flows was studied by Lyn and Altinakar (2002). The method exemplified in the simple hydrodynamic case can be extended to the Saint-Venant – Exner equations (2.18-2.20) which can be reformulated

$$\frac{\partial \mathbf{U}}{\partial t} + \frac{\partial \mathbf{F}(\mathbf{U})}{\partial x} = \frac{\partial \mathbf{U}}{\partial t} + \mathbf{A}\,\frac{\partial \mathbf{U}}{\partial x} = \mathbf{S}(\mathbf{U}) \qquad (2.132)$$

where **A** is the Jacobian matrix of the system defined as

$$\mathbf{A} = \frac{\partial\,\mathbf{F}(\mathbf{U})}{\partial \mathbf{U}} = \begin{pmatrix} u & h & 0 \\ g & u & g \\ \frac{1}{1-\varepsilon_0}\frac{\partial q_s}{\partial h} & \frac{1}{1-\varepsilon_0}\frac{\partial q_s}{\partial u} & 0 \end{pmatrix} \qquad (2.133)$$

The characteristic polynomial is

$$|\,\mathbf{A} - \lambda \mathbf{I}\,| = \lambda^3 + a_1\lambda^2 + a_2\lambda + a_3 = 0 \qquad (2.134)$$

where

$$a_1 = -2u \qquad a_2 = u^2 - gh - \frac{g}{1-\varepsilon_0}\frac{\partial q_s}{\partial u} \qquad a_3 = \frac{g}{1-\varepsilon_0}\left(u\frac{\partial q_s}{\partial u} - h\frac{\partial q_s}{\partial h}\right) \qquad (2.135)$$

The three eigenvalues λ_i of the Jacobian matrix **A,** corresponding to the celerities dx/dt of the three characteristics, are the roots of the characteristic polynomial. There is no simple exact analytical expression of the eigenvalues.

To give an idea of those celerities, the following example was analysed, inspired by Rahuel (1988): a discharge q = 16 m^3/s/m, presenting a uniform flow in a channel with mobile bed (roughness $n = 0.0277$, grain diameter $d = 0.0274$ m, $\rho_s/\rho_w = 2.65$). The solid discharge q_s is computed from the Meyer-Peter–Müller formula and the derivatives of the solid discharge $\partial q_s/\partial h$ and $\partial q_s/\partial u$ are calculated analytically.

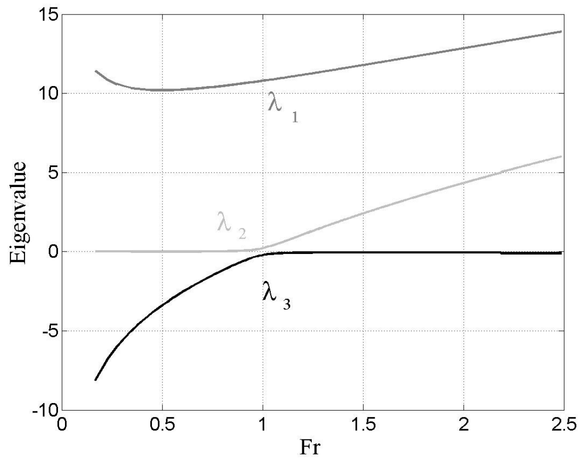

Figure 2.20. Variation of the eigenvalues with the Froude number

The three celerities are given in Figure 2.20 as a function of the Froude number. Two celerities (λ_1 and λ_2) are always positive and the third one (λ_3) is always negative.

$$\mathrm{Fr} < 1 \Rightarrow \begin{cases} \lambda_1 > 0 \\ \lambda_2 > 0 \quad (\lambda_2 \approx 0) \\ \lambda_3 < 0 \end{cases} \tag{2.136a}$$

$$\mathrm{Fr} > 1 \Rightarrow \begin{cases} \lambda_1 > 0 \\ \lambda_2 > 0 \\ \lambda_3 < 0 \quad (\lambda_3 \approx 0) \end{cases} \tag{2.136b}$$

If the solid discharge q_s does not exist (fixed bed, or mobile bed below the transport threshold), the celerities are reduced to $\lambda_{\mathrm{H1}} = u + c$ and $\lambda_{\mathrm{H2}} = u - c$ (2.122), obtained in the case of pure hydrodynamic flow (subscript H for hydrodynamics), they are compared to three eigenvalues taking sediments into account (Fig. 2.21).

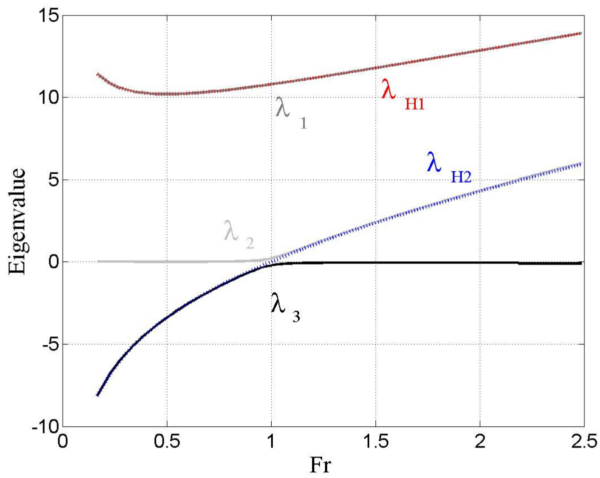

Figure 2.21. Variation of the eigenvalues with the Froude number with and without sediments

The eigenvalue λ_1 seems unaffected by the presence of sediment, as the relative difference between λ_1 and λ_{H1}

$$\Delta_{H1} = \frac{\lambda_1 - \lambda_{H1}}{\lambda_1} \tag{2.137}$$

is very small (Fig. 2.22).

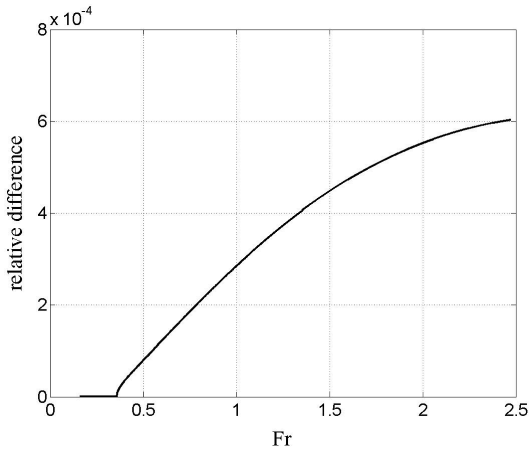

Figure 2.22. Relative difference Δ_{H1} between λ_1 and λ_{H1}

For each Froude number, the second hydrodynamic eigenvalue is spitted into two parts when sediments are present, giving λ_2 and λ_3, the sum $\lambda_2 + \lambda_3$ is close to λ_{H2}. The relative difference

$$\Delta_{H2} = \frac{(\lambda_2+\lambda_3)-\lambda_{H2}}{(\lambda_2+\lambda_3)} \tag{2.138}$$

is plotted in Figure (2.23).

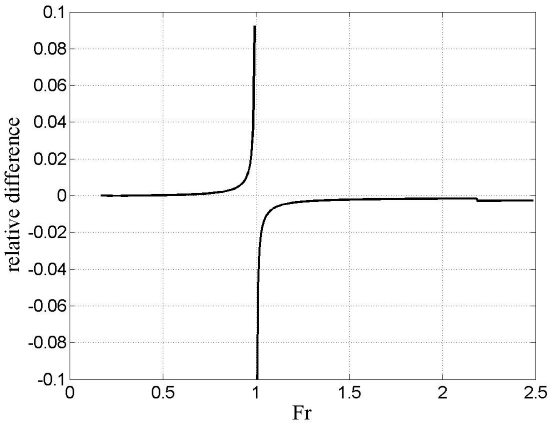

Figure 2.23. Relative difference Δ_{H2} between $(\lambda_2 + \lambda_3)$ and λ_{H2}

Under the assumption, inspired from Figures 2.22 and 2.23, $\lambda_1 = \lambda_{H1}$ and $\lambda_2 + \lambda_3 = \lambda_{H2}$, in the frame of a diploma work (Goutière and Laraichi, 2006), it was possible to find an approximated analytical expression of the eigenvalues of the Saint-Venant – Exner equations

$$\lambda_{1A} = u + c$$

$$\lambda_{2A} = \frac{1}{2}\left(u - c + \sqrt{(u-c)^2 + 4\frac{1}{(u+c)}\frac{g}{(1-\varepsilon_0)}\left(u\frac{\partial q_s}{\partial u} - h\frac{\partial q_s}{\partial h}\right)}\right)$$

$$\lambda_{3A} = \frac{1}{2}\left(u - c - \sqrt{(u-c)^2 + 4\frac{1}{(u+c)}\frac{g}{(1-\varepsilon_0)}\left(u\frac{\partial q_s}{\partial u} - h\frac{\partial q_s}{\partial h}\right)}\right)$$

(2.139a-c)

The relative differences between the approximated analytical expressions λ_{iA} of the eigenvalues and the exact values λ_i calculated numerically are

$$\Delta_1 = \frac{\lambda_1 - \lambda_{1A}}{\lambda_1} \qquad \Delta_2 = \frac{\lambda_2 - \lambda_{2A}}{\lambda_2} \qquad \Delta_3 = \frac{\lambda_3 - \lambda_{3A}}{\lambda_3} \tag{2.140}$$

These analytical solutions are close to the exact values calculated numerically as observed in Figure 2.24 where the relative differences are plotted. It was verified that these expressions remain a good approximation when applied to other flow examples. In literature, other approximated analytical solutions were proposed, for example by Lyn (1987).

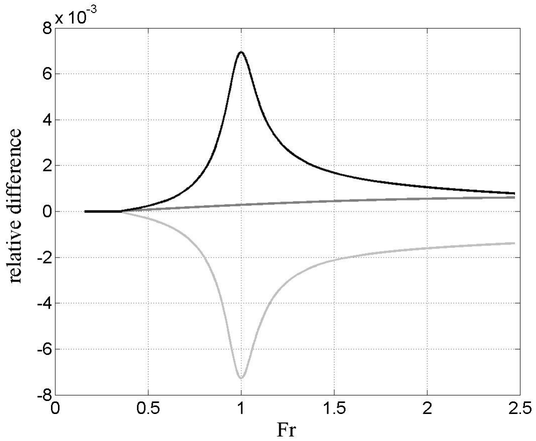

Figure 2.24. Relative difference between approximated analytical eigenvalues and exact eigenvalues — Δ_1, —Δ_2, — Δ_3

In hydrodynamics, a critical flow (Fr = 1) is characterised by the vanishing of one eigenvalue (λ_{H2}), the change in flow regime is accompanied by a change in sign of one eigenvalue. When sediments are added, the behaviour changes, none of the eigenvalue vanishes and changes its sign at Fr = 1, but the eigenvalues λ_2 and λ_3 are equal with opposite sign. Previously, Sloff (1993) suggested that the presence of the erodible bed modifies the criterion on a control section, which corresponds, in pure hydrodynamics, to a vanishing celerity (Ligett, 1993). Concerning the same topic, Sieben (1997, 1999) identified a transcritical region (0.8 < Fr < 1.2) replacing the unique critical state.

In case of subcritical flow ($\mathrm{Fr} < 1$), as λ_2 is very low , λ_3 could be assimilated to λ_{H2}, while in case of supercritical flow ($\mathrm{Fr} > 1$), as λ_3 is very low, λ_2 seems close to λ_{H2} (Fig.2.21). Except in the neighbouring of Froude number equal to one, where the presence of sediments is more influent.

This comparison between the case with and without sediment suggests that the characteristics related to λ_1 and λ_3 in subcritical case and λ_1 and λ_2 in supercritical case propagate information essentially about hydrodynamic variables h and u. Complementary, the characteristics related to λ_2 in subcritical case and λ_3 in supercritical case propagate information essentially about sediment (typically, through the variable z_b), which confirms that celerity of information in sediment is lower than in water.

This intuition has to be confronted with the three compatibility relations linked to each characteristic. The compatibility relation linked to the characteristic i is deduced from the general formulation (2.131)

$$l_{i1}\left(\frac{dh}{dt}\right)_{\lambda_i} + l_{i2}\left(\frac{du}{dt}\right)_{\lambda_i} + l_{i3}\left(\frac{dz_b}{dt}\right)_{\lambda_i} = 0 \qquad (2.141)$$

where l_{ij} the j-th component of the i-th eigenvector $\mathbf{L}_i$ linked to the eigenvalue λ_i. As exposed previously, the components of the eigenvectors i represents for each variable how much its variation propagates along the characteristic i. The variation with Froude number of the components of the left eigenvectors related to λ_1 λ_2 and λ_3 are respectively plotted in Fig 2.25 a, b and c. The three curves of each graph are related to the three variables h, u and z_b. The first characteristics (linked to λ_1) does not only concern hydrodynamic variables since the component multiplying the variation of z_b in the related compatibility relation is not negligible in comparison to the components multiplying the other variables variations (Fig. 2.25a). The characteristic related to λ_1 propagates information about the three variables. h, q and z_b. The variables whose information is propagated along the characteristics related to λ_2 and λ_3 depend on the Froude number (Fig 2.25 b and c).

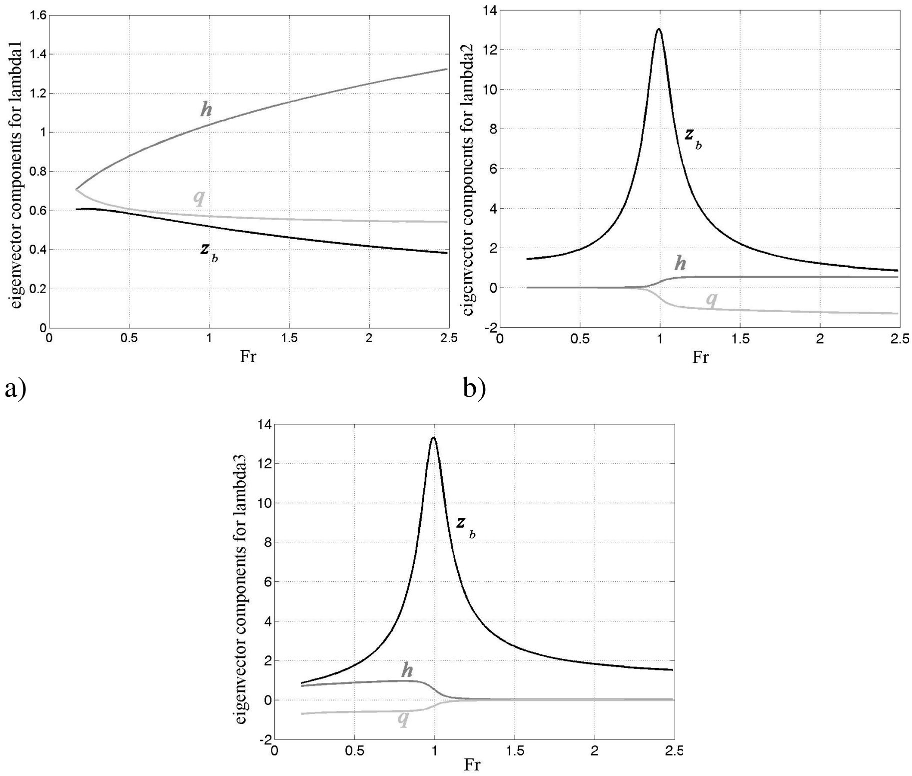

a) b)

c)

Figure 2.25. Left eigenvectors $\mathbf{L}_1$,$\mathbf{L}_2$ and $\mathbf{L}_3$ components relative to λ_1 λ_2 and λ_3

When the eigenvalues λ_2 and λ_3 are low, respectively in subcritical case and in supercritical case, the eigenvectors components multiplying the hydrodynamic variables h and q are negligible in comparison with the ones multiplying z_b, the information transmitted along the corresponding characteristics concerns mainly sediments. For other Froude numbers, around Fr = 1, in supercritical case for the λ_2-characteristic and in subcritical case for the λ_3-characteristic, all the variables are involved.

2.2.3. Two-layer model with assumptions on the velocity of the transport layer

2.2.3.1. Two-layer one-velocity model

Neglecting the source terms, the four-equation system (2.106-2.109) can be written

$$\begin{aligned}\frac{\partial \mathbf{U}}{\partial t}+\frac{\partial \mathbf{F}(\mathbf{U})}{\partial x}+\mathbf{H}(\mathbf{U})\frac{\partial \mathbf{U}}{\partial x}&=\frac{\partial \mathbf{U}}{\partial t}+\frac{\partial \mathbf{F}(\mathbf{U})}{\partial \mathbf{U}}\frac{\partial \mathbf{U}}{\partial x}+\mathbf{H}(\mathbf{U})\frac{\partial \mathbf{U}}{\partial x}\\ &=\frac{\partial \mathbf{U}}{\partial t}+\mathbf{A}(\mathbf{U})\frac{\partial \mathbf{U}}{\partial x}+\mathbf{H}(\mathbf{U})\frac{\partial \mathbf{U}}{\partial x}=\frac{\partial \mathbf{U}}{\partial t}+\mathbf{A}'(\mathbf{U})\frac{\partial \mathbf{U}}{\partial x}=0\end{aligned} \tag{2.142}$$

where $\mathbf{A}(\mathbf{U})$ is the Jacobian matrix and $\mathbf{A}'(\mathbf{U})=\mathbf{A}(\mathbf{U})+\mathbf{H}(\mathbf{U})$ a kind of pseudo-Jacobian, which reads

$$\mathbf{A}'(\mathbf{U})=\begin{pmatrix} u_m & 0 & 0 & h_m \\ 0 & u_m & 0 & h_s \\ 0 & 0 & 0 & 0 \\ \dfrac{g\,h_m}{h_m+r\,h_s} & \dfrac{g\,r\,h_s}{h_m+r\,h_s} & g & u_m \end{pmatrix} \tag{2.143}$$

The characteristic polynomial is

$$|\,\mathbf{A}'-\lambda\mathbf{I}\,|=-\lambda(u_m-\lambda)\left((u_m-\lambda)^2-\frac{grh_s^2}{h_m+rh_s}-\frac{grh_m^2}{h_m+rh_s}\right)=0 \tag{2.144}$$

The eigenvalues, which are the roots of the characteristic polynomial (2.144) can be calculated analytically (Capart, 2000)

$$\lambda_1=u_m\quad \lambda_2=u_m+\sqrt{g\frac{h_m^2+r\,h_s^2}{h_m+r\,h_s}}\quad \lambda_3=u_m-\sqrt{g\frac{h_m^2+r\,h_s^2}{h_m+r\,h_s}}\quad \lambda_4=0 \tag{2.145}$$

Four characteristics are thus obtained. For a flow in the x-direction ($u_m > 0$), it arises from (2.145) that the eigenvalues λ_1 and λ_2 are always positive while λ_4 is equal to zero (Fig. 2.26). This implies that two characteristics at least have a positive slope and one has a vertical slope in the plane (x, t). The sign of the remaining eigenvalue λ_3 depends on the flow regime. The eigenvalue λ_3 can be positive or negative.

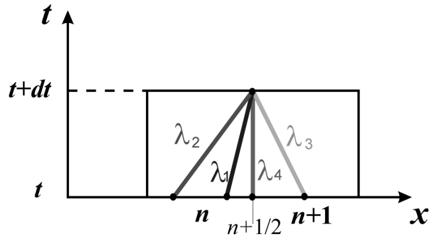

Figure 2.26. Characteristics

A kind of Froude number Fr_m linked to the mixed flow can be defined, being equal to unity when λ_3 is equal to zero:

$$\mathrm{Fr}_m = \frac{u_m}{\sqrt{g\,\dfrac{h_m^2 + r\,h_s^2}{h_m + r\,h_s}}} \tag{2.146}$$

which is nothing but the common Froude number, either if $h_s \to 0$, or if $r \to 0$.

$$\mathrm{Fr}_m < 1 \Rightarrow \begin{cases} \lambda_1 \text{ and } \lambda_2 > 0 \\ \lambda_3 < 0 \\ \lambda_4 = 0 \end{cases} \tag{2.147a}$$

$$\mathrm{Fr}_m > 1 \Rightarrow \begin{cases} \lambda_1\ \lambda_2 \text{ and } \lambda_3 > 0 \\ \lambda_4 = 0 \end{cases} \tag{2.148a}$$

The four compatibility equations may be deduced from (2.131), the matrix containing the left eigenvectors is

$$\mathbf{L} = \begin{pmatrix} -h_s & h_m & 0 & 0 \\ \dfrac{h_m\sqrt{gh'}}{h_m^2 + rh_s^2} & \dfrac{rh_s\sqrt{gh'}}{h_m^2 + rh_s^2} & \dfrac{g}{\sqrt{gh'} + u_m} & 1 \\ -\dfrac{h_m\sqrt{gh'}}{h_m^2 + rh_s^2} & -\dfrac{rh_s\sqrt{gh'}}{h_m^2 + rh_s^2} & \dfrac{g}{\sqrt{gh'} - u_m} & 1 \\ 0 & 0 & 1 & 0 \end{pmatrix} \tag{2.149}$$

The characteristic line related to the eigenvalue $\lambda_4 = 0$ is vertical. The related left eigenvector is $\mathbf{L}_4 = \begin{pmatrix}0 & 0 & 1 & 0\end{pmatrix}^{\mathrm{T}}$, the corresponding compatibility equation (2.131, with i = 4) thus reduces to

$$\left(\frac{dz_b}{dt}\right)_{\lambda 4} = 0 \tag{2.150}$$

It induces the variation of z_b with time along the vertical characteristic λ_4 to be independent of the other variables. Nevertheless, the variation of the other variables with time are dependent on z_b, non-zero eigenvectors components ($\mathbf{L}_{2,3}$ and $\mathbf{L}_{3,3}$) multiply the term relative to z_b in the compatibility relations linked to λ_2 and λ_3.

If the equation expressing the variations of z_b with time is removed from the system (2.106-2.109), identical expression of the eigenvalues (2.145) are obtained except $\lambda_4 = 0$, which disappears. The eigenvector related to λ_4 (fourth line of the matrix 2.149) and the components multiplying z_b in the compatibility relations (third column of the matrix 2.149) disappear, all the other terms of the matrix (2.149) remaining identical. In this case, information concerning z_b is neglected in the compatibility relations.

In order to compare with the other models, the eigenvalues are computed on the example inspired by Rahuel (1988) (Fig.2.27).

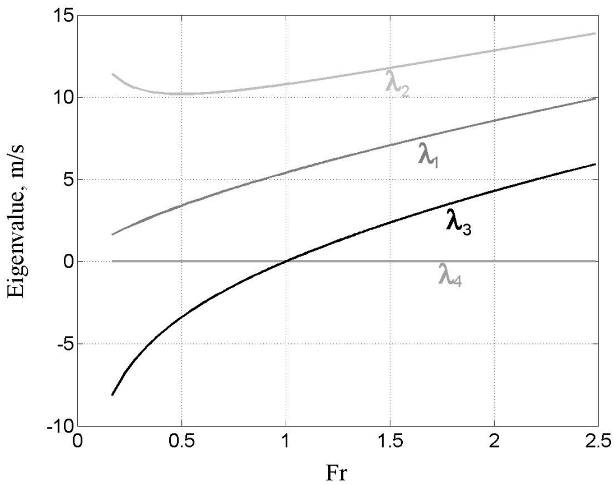

Figure 2.27. Variation of the eigenvalues with the Froude number

The eigenvalues λ_2 and λ_3 are close to pure hydrodynamic eigenvalues (2.21) even if they take the sediment transport layer into account. The non-zero additional eigenvalue λ_1 is equal to the velocity of the flow, it means the related information is transported at the velocity of the fluid.

2.2.3.2. Two-layer constant velocity ratio model

The model was adapted in order to maintain the hyperbolicity independently of the flow conditions. Neglecting the source terms, the four-equation constant velocity ratio system (2.95), (2.96), (2.97) and (2.103) can be written

$$\begin{aligned}\frac{\partial \mathbf{U}}{\partial t}+\frac{\partial \mathbf{F}(\mathbf{U})}{\partial x}+\mathbf{H}(\mathbf{U})\frac{\partial \mathbf{U}}{\partial x}&=\frac{\partial \mathbf{U}}{\partial t}+\frac{\partial \mathbf{F}(\mathbf{U})}{\partial \mathbf{U}}\frac{\partial \mathbf{U}}{\partial x}+\mathbf{H}(\mathbf{U})\frac{\partial \mathbf{U}}{\partial x}\\&=\frac{\partial \mathbf{U}}{\partial t}+\mathbf{A}(\mathbf{U})\frac{\partial \mathbf{U}}{\partial x}+\mathbf{H}(\mathbf{U})\frac{\partial \mathbf{U}}{\partial x}=\frac{\partial \mathbf{U}}{\partial t}+\mathbf{A}'(\mathbf{U})\frac{\partial \mathbf{U}}{\partial x}=0\end{aligned} \tag{2.151}$$

where $\mathbf{A}(\mathbf{U})$ is the Jacobian matrix and $\mathbf{A}'(\mathbf{U}) = \mathbf{A}(\mathbf{U}) + \mathbf{H}(\mathbf{U})$ a kind of pseudo-Jacobian, which reads

$$\mathbf{A}'(\mathbf{U}) = \begin{pmatrix} u_w & 0 & 0 & h_w \\ 0 & \alpha u_w & 0 & \alpha h_s \\ 0 & 0 & 0 & 0 \\ \xi & \dfrac{\rho_w g h_w + \rho_s' g h_s}{\rho_w h_w + \alpha \rho_s' h_s} & \xi & \dfrac{\rho_w h_w + \alpha^2 \rho_s' h_s}{\rho_w h_w + \alpha \rho_s' h_s} u_w \end{pmatrix} \tag{2.152}$$

The characteristic polynomial writes

$$|\mathbf{A}' - \lambda \mathbf{I}| = \lambda \left(a\lambda^3 + b\lambda^2 + c\lambda + d \right) = 0 \tag{2.153}$$

Where the four eigenvalues have no simple analytical solution. The polynomial is numerically solved in order to find the four eigenvalues. Two of the eigenvalues are always positive and one is always equal to zero, the sign of the remaining eigenvalue depends on the flow conditions. When the sign of this last eigenvalue changes, the product of the three non-zero eigenvalues is then equal to zero.

$$\begin{aligned} \prod_{i=1}^{3} \lambda_i = \frac{d}{a} = u_w^2 \left(\rho_w h_w + \alpha^2 \rho_s' h_s \right) - c_w^2 \left(\rho_w (h_w + h_s) \right) \\ - c_s^2 \left(\rho_w h_w + \rho_s' h_s \right) = 0 \end{aligned} \tag{2.154}$$

with $c_w = \sqrt{g\, h_w}$ and $c_s = \sqrt{g\, h_s}$. The control section is then characterised by a kind of mixed Froude number

$$\mathrm{Fr}_{sw} = \frac{u_w^2 \left(\rho_w h_w + \alpha^2 \rho_s' h_s \right)}{c_w^2 \left(\rho_w (h_w + h_s) \right) + c_s^2 \left(\rho_w h_w + \rho_s' h_s \right)} = 1 \tag{2.155}$$

If there is no sediment transport ($h_s = 0$), the mixed Froude number Fr_{sw} reduce to the water Froude number Fr_w. Identically, if all the depth is occupied by the transport layer and no clear water remains ($h_w = 0$), the mixed Froude number Fr_{sw} reduce to the sediment Froude number Fr_s. When

$\mathrm{Fr}_{sw} < 1$, (2.154) is negative implying one of the eigenvalues is negative. If $\mathrm{Fr}_{sw} > 1$, all the non-zero eigenvalues are positive.

$$\mathrm{Fr}_{sw} < 1 \Rightarrow \begin{cases} \lambda_1 \text{ and } \lambda_2 > 0 \\ \lambda_3 < 0 \\ \lambda_4 = 0 \end{cases} \tag{2.156}$$

$$\mathrm{Fr}_{sw} > 1 \Rightarrow \begin{cases} \lambda_1\ \lambda_2 \text{ and } \lambda_3 > 0 \\ \lambda_4 = 0 \end{cases} \tag{2.157}$$

In order to compare with the other models, the eigenvalues are computed on the example inspired from Rahuel (1988) (Fig.2.28) for a velocity ratio $\alpha = 0.3$.

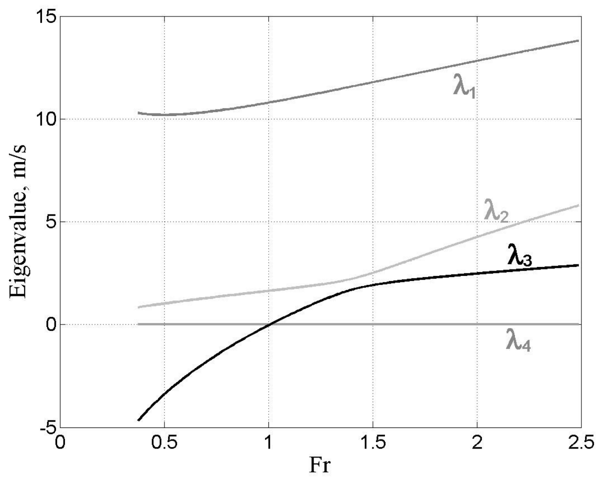

Figure 2.28. Variation of the eigenvalues with the Froude number

Even if sediments are taken into account, the eigenvalue λ_1 is close to the pure hydrodynamic eigenvalue $u_w + c_w$. As it is the case for the Saint-Venant – Exner equations, the eigenvalues λ_2 and λ_3 seem to be compound of two parts, in this example the change between the two parts occurs around $\mathrm{Fr}_w = 1.4$. The part of the eigenvalue λ_2, corresponding to $\mathrm{Fr}_w > 1.4$, and the part of λ_3, corresponding to $\mathrm{Fr}_w < 1.4$ are close to the hydrodynamic eigenvalue $u_w - c_w$. The remaining part of the eigenvalues λ_2 and λ_3 is strongly affected by a change of the velocity ratio α. Variations of the other eigenvalues due to a change in the velocity ratio are negligible, nevertheless it influences the value of the Froude number delimiting the two parts of the eigenvalues λ_2 and λ_3. The delimiting Froude number increases with the velocity ratio. If the velocity ratio $\alpha = 1$, the velocity is identical in both layers, the eigenvalues are the same than those calculated with the one-velocity model plotted in Figure 2.27.

2.2.4. Two-layer two-velocity model

Neglecting the source terms, the five-equation system (2.73-2.77) can be written

$$\begin{aligned}\frac{\partial \mathbf{U}}{\partial t}+\frac{\partial \mathbf{F}(\mathbf{U})}{\partial x}+\mathbf{H}(\mathbf{U})\frac{\partial \mathbf{U}}{\partial x}&=\frac{\partial \mathbf{U}}{\partial t}+\frac{\partial \mathbf{F}(\mathbf{U})}{\partial \mathbf{U}}\frac{\partial \mathbf{U}}{\partial x}+\mathbf{H}(\mathbf{U})\frac{\partial \mathbf{U}}{\partial x}\\&=\frac{\partial \mathbf{U}}{\partial t}+\mathbf{A}(\mathbf{U})\frac{\partial \mathbf{U}}{\partial x}+\mathbf{H}(\mathbf{U})\frac{\partial \mathbf{U}}{\partial x}=\frac{\partial \mathbf{U}}{\partial t}+\mathbf{A}'(\mathbf{U})\frac{\partial \mathbf{U}}{\partial x}=0\end{aligned} \tag{2.158}$$

where $\mathbf{A}(\mathbf{U})$ is the Jacobian matrix and $\mathbf{A}'(\mathbf{U})=\mathbf{A}(\mathbf{U})+\mathbf{H}(\mathbf{U})$ a kind of pseudo-Jacobian, which reads

$$\mathbf{A}'(\mathbf{U})=\begin{pmatrix}0&0&0&1&0\\0&0&0&0&1\\0&0&0&0&0\\-u_w^2+gh_w&gh_w&gh_w&2u_w&0\\\frac{\rho_w}{\rho_s'}gh_s&-u_s^2+gh_s&gh_w&0&2u_s\end{pmatrix} \tag{2.159}$$

For this five-equation system the eigenstructure has no straightforward analytical solution, and it is impossible to express the compatibility equations linked to the characteristics. Thus the eigenvalues of the pseudo-Jacobian matrix **A'** (2.159) are computed numerically.

To explore the signs of the eigenvalues, two theoretical examples were computed. In the first example, the water depth h_w was supposed to vary from a low ($h_w = h_s = 0.01\,\mathrm{m}$) to a high value, while the other parameters were fixed: the bed level z_b, the velocities u_w and u_s in each layer and the transport-layer thickness h_s. The water Froude number $\mathrm{Fr}_w = u_w / \sqrt{g\, h_w}$ thus decreases since u_w is fixed and h_w increases. It is possible to represent the eigenvalues as a function of this Froude number (Fig. 2.29). The smallest eigenvalue becomes negative for water Froude numbers lower than 1.1, showing that the water Froude number alone is not sufficient to determine the sign of the eigenvalues and thus to characterise the flow regime. It can be seen that for lower water Froude numbers the five eigenvalues are real and distinct, while for higher values, two of them become conjugate complex (same real part, opposite imaginary part). In this specific example, the problem loses its hyperbolic character only for rather high water Froude numbers, in supercritical regime. Such a loss of hyperbolicity, already pointed out by LeVeque (2002) was recently also mentioned, in the case of a two-layer shallow flow model, by Audusse (2005) and Spinewine (2005).

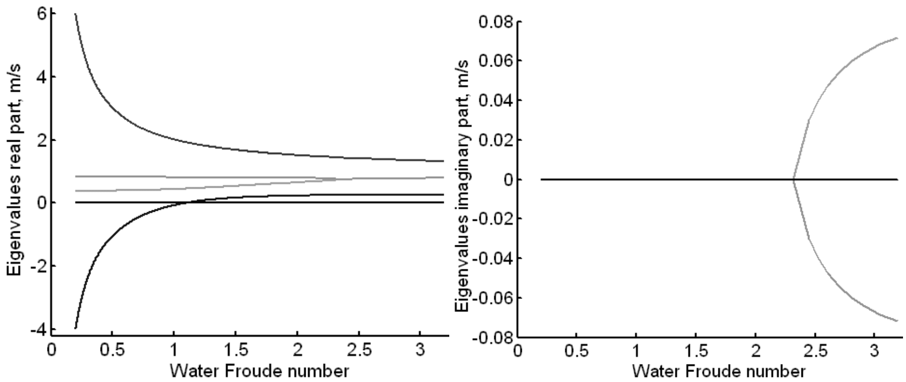

a) b)

Figure 2.29. Eigenvalues function of water Froude number Fr_w, a) real and b) imaginary part. u_w = 1 m/s, u_s = 0.6 m/s, h_s = 0.01 m and h_w varies from 0.01 to 2.55 m

In the second example (Fig. 2.30), the transport thickness h_s is larger (0.10 m instead of 0.01 m), for the considered range of water Froude numbers, the eigenvalues are real. One eigenvalue is always negative and for water Froude numbers lower than 0.5, a second one becomes negative.

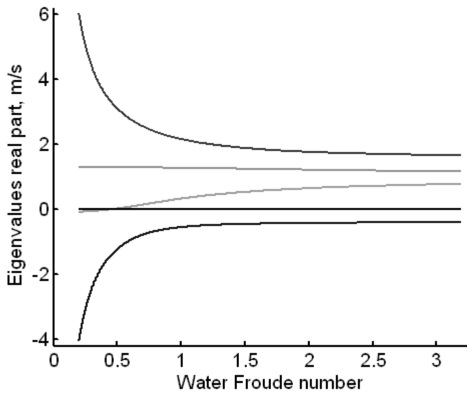

Figure 2.30. Eigenvalues function of water Froude number Fr_w, real part. u_w = 1 m/s, u_s = 0.6 m/s, h_s = 0.1 m and h_w varies from 0.01 to 2.55 m

It was observed that (1) one of the celerities was zero as in the 4-equation case; (2) the two extreme characteristics have a real celerity; and (3) the two intermediate eigenvalues may have an imaginary part, depending on the flow conditions. Thus, the system may become non hyperbolic in some cases.

These observations can be specified using properties of the characteristic polynomial form:

$$\left|\mathbf{A}'-\lambda\mathbf{I}\right|=0 \quad\Rightarrow\quad \lambda\left(a\lambda^4+b\lambda^3+c\lambda^2+d\lambda+e\right)=0 \qquad (2.160)$$

If the non-zero roots are $\lambda_i, i=1\ldots4$, the sum and the product of those eigenvalues are respectively:

$$\sum_{i=1}^{4}\lambda_i=\lambda_1+\lambda_2+\lambda_3+\lambda_4=-\frac{b}{a} \qquad \prod_{i=1}^{4}\lambda_i=\lambda_1\lambda_2\lambda_3\lambda_4=\frac{e}{a} \quad (2.161\text{ a-b})$$

Both the sum and the product are real, which implies that if two roots became complex they would be conjugate in such a way that the product of them would be positive. To analyse the sign of the eigenvalues, the product (2.161 b) may be written:

$$\prod_{i=1}^{4}\lambda_i=c_s^2\,c_w^2\left(1-\frac{\rho_w}{\rho_s'}\right)+u_s^2\,u_w^2-\left(c_w^2\,u_s^2+c_s^2\,u_w^2\right) \qquad (2.162)$$

with $c_w = \sqrt{g\,h_w}$ and $c_s = \sqrt{g\,h_s}$. The sign of the non-zero eigenvalue product (2.162), and thus of the characteristics, changes when

$$Z_{sw} = \frac{c_s^2\, c_w^2 \left(1 - \frac{\rho_w}{\rho_s'}\right) + u_s^2\, u_w^2}{c_w^2\, u_s^2 + c_s^2\, u_w^2} = \frac{\left(1 - \frac{\rho_w}{\rho_s'}\right) + \mathrm{Fr}_s^2\, \mathrm{Fr}_w^2}{\mathrm{Fr}_s^2 + \mathrm{Fr}_w^2} = 1 \quad (2.163)$$

where $\mathrm{Fr}_s = u_s / c_s$ is the sediment Froude number. The function Z_{sw} is a kind of two-layer Froude number describing the interference between water and sediment wave celerities. If $Z_{sw} > 1$, the number of negative characteristics is even (0, 2 or 4 negative characteristics) while if $Z_{sw} < 1$, this number is odd (1 or 3 negative characteristics). If the transport layer vanishes ($h_s \to 0$), Z_{sw} becomes equivalent to the square of the water Froude number Fr_w. If the water layer disappears ($h_w \to 0$), Z_{sw} becomes equivalent to the square of the sediment Froude number Fr_s. If $Z_{sw} = 1$ there is a kind of control section, which corresponds to a relation between the depths (h_w and h_s) and the discharges ($h_w u_w$ and $h_s u_s$) in each layer.

Merging the above considerations to the physics of the problem, it is possible to determine the sign of the eigenvalues, and thus also the number of boundary conditions required at a boundary of the problem.

One eigenvalue is always equal to zero. The corresponding characteristics is thus vertical (x = constant) and the associated compatibility equation reads

$$\frac{dz_b}{dt} = 0 \quad (2.164)$$

At least two of the four other eigenvalues are positive. This results from computations but also from physics: amongst the five variables, the discharges q_w and q_s are essentially depending on upstream conditions, implying positive 'associated' characteristics.

The sign of the two remaining eigenvalues is depending on both the water Froude number Fr_w and the two-layer Froude number Z_{sw}, according to Table 2.1. If the flow is subcritical ($\mathrm{Fr}_w < 1$) the water depth h_w is a downstream condition and the 'associated' characteristic is negative, while the water depth is an upstream condition and the characteristic positive if the flow is supercritical ($Fr_w > 1$). The sign of the last eigenvalue may be deduced from the two-layer Froude number Z_{sw}, leading to an even or an odd number of negative characteristics.

	$Z_{sw} > 1$ (even number of negative)	$Z_{sw} < 1$ (odd number of negative)
$Fr_w > 1$ (at least 3 positive)	+ + + + 0 (case A)	+ + + 0 – (case B)
$Fr_w < 1$ (at least 1 negative)	+ + 0 – – (case C)	+ + + 0 – (case D)

Table 2.1. Sign of the five eigenvalues and 'associated' characteristics

It can be shown that the relation between the two-layer Froude number Z_{sw} and the water Froude number Fr_w is not evident. Generally, the value of the water Froude number Fr_w corresponding to $Z_{sw} = 1$, is also close to 1, in such a way that range of application of cases B and C are rather limited in actual cases.

Spinewine (2005) studied the flow conditions under which the system becomes non hyperbolic. He exposed some recent results obtained by Audusse (2005) in simplified cases. In the specific case of two fluids of same density $\rho_s' = \rho_w$, flowing on a horizontal bed $\partial z_b / \partial x = 0$, this author proposes an analytical first-order approximation of the eigenvalues, two of them possibly being complex. According to his results, the imaginary part disappears either when the velocity is the same in each layer ($u_s = u_w$, like in the one-velocity model) or when the lower layer is relatively thin in comparison to the upper layer ($h_s << h_w$). In more general conditions, Lawrence (1990) proposed an analytical solution for the eigenvalues, but those expressions are too complicated, which makes them difficult to interpret. Nevertheless he defined the discriminant *D* depending on the flow parameters, the sign of the discriminant changes when the internal eigenvalues become complex.

$$D\left(\frac{u_w - u_s}{\sqrt{g(h_w + h_s)}}, \frac{h_w}{h_w + h_s}, \frac{\rho_w}{\rho_s'}\right) = \prod_{\substack{i,j=1 \\ i<j}}^{4} (\lambda_i - \lambda_j)^2 \qquad (2.165)$$

The locus corresponding to D = 0, determines the boundary between the hyperbolic and non-hyperbolic state. The locus corresponding to several density ratios ρ_s'/ρ_w is plotted by Spinewine (2005). Lower and closer to 1 the density ratio is, wider is the non-hyperbolic domain. It implies that when the concentration in the transport layer is lower than the concentration in the bed, the volumetric mass of the transport layer being closer to the volumetric mass of water, the non-hyperbolic domain is wider. The non-hyperbolic domain also becomes wider when the velocity ratio u_s / u_w becomes smaller, while, when the velocity is identical in both layers (like in the one-velocity model), the problem is hyperbolic whatever are the other flow conditions.

In order to compare with the other models, the eigenvalues are calculated on the basis of the example proposed by Rahuel (1988) (Fig.2.31). The internal eigenvalues are complex for a wide range of Froude numbers ($1<Fr_w<2.25$). As they are conjugate complex, the real part of both eigenvalues is identical, no discontinuity is observed in the real part when the internal eigenvalues enter or leave the non-hyperbolic region.

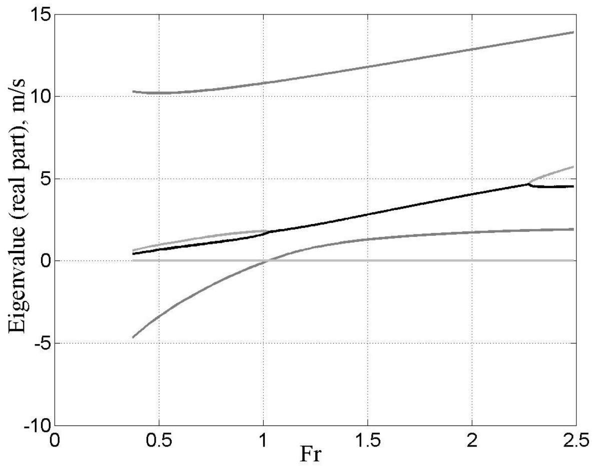

a)

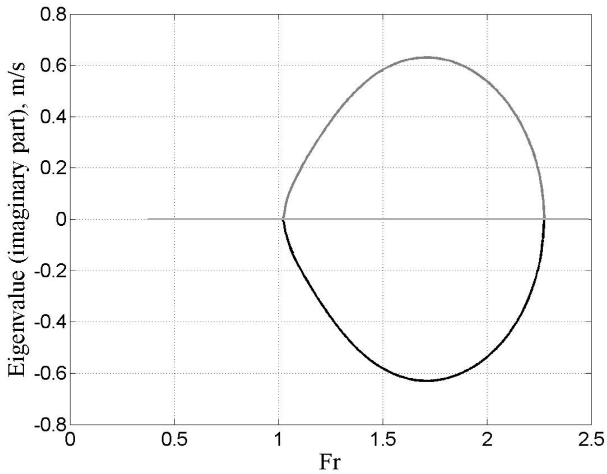

b)

Figure 2.31. Variation of the eigenvalues with the Froude number a) real part b) imaginary part